Received: 29 August 2023 | Revised: 16 November 2023 | Accepted: 7 January 2024

DOI: 10.1002/apj.3031

RESEARCH ARTICLE

Asia-Pacific Journal of Chemical Engineering | Curtin University | WILEY

Application of PC-SAFT EoS and SCFT for the modeling of thermophysical properties comprising deep eutectic solvent and alcohols

Ncomeka Mgxadeni[1] | **Bakusele Kabane**[2] | **Ariel Hernández**[3] | **Indra Bahadur**[1] | **Faruq Mohammad**[4] | **Ahmed Abdullah Soleiman**[5] | **Hamed Hashemi**[6] | **Mwadham M. Kabanda**[7]

[1]Department of Chemistry, North-West University (Mafikeng Campus), Private Bag X2046, Mmabatho, South Africa

[2]Physical Chemistry Laboratories, Department of Chemistry, Durban University of Technology (ML-Sultan Campus), Durban, South Africa

[3]Departamento de Ingeniería Industrial, Facultad de Ingeniería, Universidad Católica de la Santísima Concepción, Concepción, Chile

[4]Department of Chemistry, College of Science, King Saud University, Riyadh, Kingdom of Saudi Arabia

[5]Department of Chemistry, Southern University and A&M College, Baton Rouge, Louisiana, USA

[6]Department of Chemical and Metallurgical Engineering, University of the Witwatersrand, Johannesburg, South Africa

[7]Department of Chemistry, School of Mathematical and Natural Sciences, University of Venda, Thohoyandou, South Africa

Correspondence
Indra Bahadur, Department of Chemistry, North-West University (Mafikeng Campus), Private Bag X2046, Mmabatho 2735, South Africa.
Email: bahadur.indra@nwu.ac.za

Funding information
North-West University, Materials Science Innovation & Modelling Research Focus Area (MaSIM); National Research Fund (NRF); Sasol and Chemical Industries Educational and Training Authority (CHIETA); King Saud University, Grant/Award Number: RSP2024R355

Abstract

Zinc (II) chloride based deep eutectic solvent (DES) were formed by mixing zinc (II) chloride with phosphoric acid. Fourier-transform infrared spectroscopy was used to identify any possible shifts when the two compounds were assorted, and differential scanning calorimetry (SDT Q600 V20.9 Build 2D) was utilized to evaluate the formation of deep eutectic solvent. Densities, ρ, and speed of sound, u, of [$ZnCl_2$][phosphoric acid] 1:2.5 with methanol, ethanol, or propanol have been measured at $T = (293.15, 303.15, 308.15, \text{and } 313.15)$ K and at atmospheric pressure. Excess molar volumes (V_m^E), isentropic compressibilities (κ_s), deviation in isentropic compressibility ($\Delta\kappa_s$), and intermolecular free length (L_f) were calculated from the densities, and speed of sound, respectively. To fit the excess molar volumes and deviation in isentropic compressibilities, the Redlich–Kister smoothing polynomial was used. Also, we have used perturbed chain statistical associating fluid theory equation of state (PC-SAFT EoS) for modeling the densities of the binary mixtures, and Schaaff's collision factor theory (SCFT) and Nomoto's relation (NR) were used for modeling the speed of sounds for the binary mixtures.

KEYWORDS

PC-SAFT EoS, Schaaff's collision factor theory, thermophysical properties, zinc (II) chloride based DESs

1 | INTRODUCTION

Zinc (II) chloride-based deep eutectic solvents (DESs) are a type of ionic liquid formed by combining a metal salt (such as zinc chloride) with a hydrogen bond donor (such as acetic acid or phosphoric acid) and so on.[1] DESs have gained significant attention in recent years due to their unique properties in metallurgy, electrodeposition, gas separation, gas capture, power systems, battery technology, bio-catalysis, biomass processing, pharmaceutical and medical research, organic synthesis, nanomaterials synthesis, and functionalization.[2–4] Because of their tunability to optimize solubility, viscosity, selectivity, and other physicochemical properties for a specific application, DESs are emerging as a new class of sustainable solvents.[2,5] They are generally considered renewable, inexpensive, and green 'designer' solvents. They are marketed as eco-friendly alternatives to a wide range of conventional solvents.[2,6,7]

Therefore, the study and understanding of the properties of DESs are prerequisites for developing their potential as new solvents. Designing new processes and products based on these chemical species requires a fundamental understanding of the thermophysical properties. Thermophysical properties refer to the physical characteristics of a substance, such as its density, speed of sound, refractive index, viscosity, and conductivity.[8–10] In addition to offering key details to describe the nature of intermolecular forces, experimental data on density, and speed of sound across a wide range of pressure and temperatures can also produce useful applications in industrial domains like chemical reactors or separation procedures. Thermodynamic properties, on the other hand, describe the relationships between a substance's physical properties and its energy content.[11] These properties can provide insights into the thermodynamic driving forces behind the formation of these mixtures and can be used to optimize the design of chemical processes that use these solvents and their applications.[11]

According to the literature review, ZnCl (II) has previously been used as a water-in-salt electrolyte for a dendrite-free Zn metal anode, making it an ideal component for DESs used as zinc ion battery electrolytes.[12,13] Furthermore, preliminary reports suggest that ZnCl (II)-based DESs have a wide range of potential applications due to their unique properties, such as low toxicity, biodegradability, low cost, and high stability.[14,15] Here are some examples of the potential applications of ZnCl (II)-based DES. Cellulose processing: ZnCl (II)-based DESs can dissolve cellulose and other polysaccharides, making them potentially useful in the production of biofuels, pharmaceuticals, and other products derived from biomass.[16] Energy storage: ZnCl (II)-based DESs have been investigated as electrolytes for electrochemical energy storage devices such as supercapacitors and batteries. They have shown promising performance in terms of electrochemical stability, high conductivity, and low cost.[17] Chemical synthesis: ZnCl (II)-based DESs can be used as reaction media for various chemical reactions, including organic synthesis and catalysis. They are effective in promoting reactions such as esterification, Friedel–Crafts acylation, and Heck coupling.[18] Mgxadeni et al (2022) used GLC to assess ([$ZnCl_2$][Acetic acid] 1:4 and ([$ZnCl_2$][phosphoric acid]) 1:2.5 DES as a possible separating agent for various organic solutes at temperatures ranging from $T = (313.15–353.15)$.[19] ZnCl (II)-based DESs have shown great potential in various fields, and their development and applications continue to be an active area of research.

In this instance, phosphoric acid (H_3PO_4) is a triprotic acid, meaning it has three ionizable hydrogen atoms that can donate a proton (H^+) to form hydrogen bonds.[20–22] As a result, phosphoric acid can act as a hydrogen bond donor in various biological and chemical applications. For example, it is used as a buffer in biological systems, where it helps to maintain a stable pH by acting as both an acid and a base. It is also used in the production of fertilizers, detergents, and food additives.[23–25]

To the best of our knowledge, no data have been published previously on binary systems of ([$ZnCl_2$][phosphoric acid] 1:2.5 + methanol), ([$ZnCl_2$][phosphoric acid] 1:2.5 + ethanol), and ([$ZnCl_2$][phosphoric acid] 1:2.5 + propanol). In this article, we attempt to explain the ion-solvent or solute-solvent interactions between ([$ZnCl_2$][phosphoric acid] 1:2.5 and solvents: methanol, ethanol, and propanol, at $T = 293.15$ K, 303.15 K, 308.15 K, and 313.15 K using excess molar volume, deviation in isentropic compressibility and intermolecular free length, which have been calculated from the experimental data of density, and speed of sound respectively. Data on excess molar volume and deviation in isentropic compressibility were fitted using the Redlich–Kister smoothing polynomial.[26]

Alcohols are strongly linked together by hydrogen bonds.[27] In the study of the behavior interaction of alcohols with other solvents, these self-associated dependencies of temperature, chain length, and position of the OH group are crucial parameters.[28] To better understand solvation behavior, examining the thermophysical characteristics of mixtures containing DES and alcohols is crucial.[29] The information from this mixture's excess thermodynamics properties will be very helpful and comprehensive in understanding the intermolecular and structural interactions.[30] Since DES is still an unknown solvent and alcohols are the most popular solvents used in chemical reactions and numerous industrial processes,

TABLE 1 Molecular mass, suppliers, CAS number, and purity of chemicals used.

Chemical name	Molecular mass (g/mol)	Supplier	CAS number	Mass fraction purity
Zinc chloride	136.30	Merck	7646-85-7	≥ .99
Phosphoric acid	97.994	Sigma-Aldrich	7664-38-2	≥ .99
Methanol	32.04	Sigma-Aldrich	67-56-1	≥ .99
Ethanol	46.07	Sigma-Aldrich	64-17-5	≥ .99
Propanol	60.1	Sigma-Aldrich	71-23-8	≥ .99

the mixture of DES + alcohols are an intriguing liquid system for studying molecular interactions. In this work, we have used perturbed chain statistical associating fluid theory equation of state (PC-SAFT EoS) for modeling the density of DES + alcohols, using DES as pseudo-pure component approach, while the speed of sound for the binary mixtures was predictively modeled from the combination between EoS + SCFT and EoS + NR.

2 | EXPERIMENTAL SECTION

2.1 | Materials

Zinc chloride, phosphoric acid, methanol, ethanol, and propanol were purchased from Sigma-Aldrich. The purity of these substances was >.99 (mass fraction) as presented in Table 1. All samples were prepared just before measurements to prevent compositional variations due to solvent evaporation. No additional purification procedures were used in the preparation of any of the sample mixtures.

Table 2 compares the experimental density, ρ, and speed of sound, u, values determined in the current study to those reported in the literature for pure solvents at $T = (293.15, 303.15, 308.15, \text{and } 313.15)$ K. The selected alcohol's properties values are in good agreement with those reported in the literature.

2.2 | Apparatus and procedure

Preparation of the investigated DESs involves the mixing of at least one hydrogen bond acceptor (HBA) and one hydrogen bond donor (HBD) compound. HBAs can be either organic salts or metal salts whereas HBDs can be metal salt hydrate, alcohols, carboxylic acids, polyanalines A detailed preparation of [$ZnCl_2$][phosphoric acid] 1:2.5 has been described in our previous work[1] as shown in Figure 1. The prepared solvent was characterized by using Fourier-transform infrared spectroscopy was used to identify any possible shifts when the two compounds were assorted, and this is shown in Figure 2. This was further confirmed by using NMR shown in Figure S1. Differential scanning calorimetry (SDT Q600 V20.9 Build 2D) was utilized to evaluate the formation of deep eutectic solvent, and the observed temperature was approximately 30°C, below the melting point of the individual compound used for the preparation of the investigated solvent and the results are shown in Figure 3. In addition, the prepared solvent was purified to eliminate any unwanted material and the content of was determined by using Karl–Fischer and was found to be less than 309.10^{-6}%.

The experimental procedure used to determine the density and speed of sound using the DSA 5000 M method has been extensively reported in the literature.[51–53] Masses of the constituents of the binary mixtures were determined using an OHAUS analytical balance with a precision of .0001 g. The uncertainty of the mole fraction was .0006. To prevent evaporation during the preparation of the binary mixtures, the pure liquids were placed into shelled vials. The mixtures were then shaken to ensure that all the samples were thoroughly mixed.

An Anton Paar DSA 5000 M vibrating U-tube densimeter, calibrated to the experimental temperatures with a precision of .02 K, was used to measure the density and sound speed. The sound velocity was determined at a frequency of 3 MHz.[54] The ultrapure water was used to calibrate the instruments. The uncertainties were estimated for density and speed of sound measurements within .0009 g·cm^{-3} and 2.63 m·s^{-1}, respectively.

3 | THEORETICAL MODELS

3.1 | Density

PC-SAFT EoS can be written in terms of the Helmholtz energy (A), which is the sum of four contributions, i.e., ideal gas contribution (A^{id}), a hard-chain contribution (A^{hc}), attractive interactions of dispersion forces (A^{disp}), and association contribution (A^{assoc}). Therefore, PC-SAFT EoS is given by Equation (1):

TABLE 2 Comparison of experimental and literature density, ρ,, and speed of sound, u, of pure components at $T = (293.15, 303.15, 308.15, 313.15, \text{and } 313.15)$ K and at .1 MPa.

	ρ (g·cm^{-3})		u (m·s^{-1})	
T (K)	expt	lit	expt	lit
Methanol				
293.15	.7916	.7961[31]	1119.60	1119.00[31]
		.7913[32]		1119.13[32]
		.7936[33]		1106.63[33]
		.7914[34]		
		.7930[35]		
		.7926[36]		1105.19[36]
		.7910[37]		1119.60 [37]
		.7912[38]		
		.7910[39]		1120.00[39]
303.15	.7822	.7819[34]	1087.20	
		.7819[32]		1086.00[32]
		.7819[40]		1086.00[40]
		.7846[33]		1082.73[33]
		.7837[36]		1088.73[36]
		.7824[41]		1092.29[41]
		.7827[42]		1088.26[42]
		.7836[35]		
		.7810[43]		1085.89 [43]
		.7820[37]		1086.60[37]
		.7818[38]		
		.7820[39]		1087.00[39]
308.15	.7776	.7772[34]	1071.07	
		.7772 [32]		1069.70[32]
		.7779[33]		1068.82[33]
		.7769[36]		1070.82[36]
		.7771[40]		1069.00 [40]
		.7776[41]		1077.90[41]
		.7779[42]		1072.04[42]
		.7773[43]		1074.00 [43]
		.7771[38]		
313.15	.7727	.7741[35]	1055.00	
		.7724[32]		1053.57[32]
		.7724[33]		1059.41[33]
		.7720[37]		1054.20[37]
		.7725[40]		1052.00[40]
		.7729[41]		1065.03[41]
		.7732[42]		1055.91[42]
		.7728[43]		1052.00[43]
		.7723[38]		
		773.00[39]		
Ethanol				
293.15	.7896	.7894[44]	1160.37	
		.7897[32]		1161.00[32]
		.7894[33]		1159.34[33]
		.7895[34]		
		.7895 [36]		1161.38[36]
		.7895[45]		1162.30[45]
		.7895[35]		
		.7896[37]		1162.30[37]
		.7895[38]		
		.7900[39]		1162.00[39]
303.15	.7810	.7808[44]	1126.91	
		.7810[32]		1126.77[32]
		.7820[33]		
		.7808[34]		
		.7820[36]		1129.01[36]
		.7810[40]		1127.00[40]
		.7809[45]		1128.90[45]
		.7810[46]		
		.7820[47]		1128.00[47]
		.7809[35]		
		.7810[37]		1128.20[37]
		.7807[38]		
		.7810[39]		1127.00[39]
		.7820[43]		1128.00[43]
308.15	.7723	.7764[44]	1109.94	
		.7767[32]		1109.87[32]
		.7778[36]		1099.74[36]
		.7755[40]		1109.00[40]
		.7777[47]		1098.00[47]
		.7764[38]		
		.7777[43]		1098.00[43]
313.15	.7701	.7720[44]	1093.40	
		.7723[32]		1093.11[32]
		.7732[33]		1090.92[33]
		.7722[34]		
		.7732[36]		1093.11[36]
		.7723[40]		1089.00[40]
		.7722[45]		1095.40[45]
		.7722[46]		
		.7736[47]		1086.00[47]

(Continues)

TABLE 2 (Continued)

	ρ (g·cm^{-3})		u (m·s^{-1})	
T (K)	expt	lit	expt	lit
		.7722[35]		
		.7720[37]		1094.50[37]
		.7721[38]		
		.7720[39]		1094.00[39]
		.7736[43]		1086.00[43]
Propanol				
293.15	.8036	.8036[48]	1222.69	
		.8036[32]		1223.12[32]
		.8037[36]		1196.64[36]
		.8038[44]		
		803.75[34]		
		.8030[49]		1224.30[49]
		.8039 [46]		
		.8039[35]		
		.8036[38]		
		.8040[39]		1226.00[39]
303.15	.7956	.7955[50]	1188.88	
		.7956[32]		1188.64[32]
		.7960[42]		1189.26[42]
		.7956[48]		
		.7956[44]		
		.7957[36]		1185.89 [36]
		.7955[34]		
		.7960[49]		1189.90[49]
		.7958[35]		
		.7956[38]		
		.7960[39]		1191.00[39]
308.15	.7916	.7915[48]	1171.93	
		.7915[32]		1171.64[32]
		.7905[36]		1170.01[36]
		.7919[42]		1172.37[42]
		.7915[44]		
		.7915[38]		
313.15	.7875	.7874[50]	1155.23	
		.7874[32]		1154.88[32]
		.7874[36]		1159.51[36]
		.7878[42]		1155.53[42]
		.7874[48]		
		.7874[44]		
		787.42[34]		
		.7880[49]		1156.00[49]
		.7874[46]		

(Continues)

TABLE 2 (Continued)

	ρ (g·cm^{-3})		u (m·s^{-1})	
T (K)	expt	lit	expt	lit
		.7876[35]		
		.7874[38]		
		.7880[39]		1157.00[39]

Note: Standard uncertainties u are $u(T) = .02$ K, $u(p) = .04$ MPa, and the combined expanded uncertainties Uc in mole fraction, density, andspeed of sound were $Uc(x) = .0006$, $Uc(\rho) = .0009$ g·cm^{-3}, $Uc(\underline{u}) = 2.63$ m·s^{-1}, respectively (.95 level of confidence).

$$A = A^{id} + A^{hc} + A^{disp} + A^{assoc} \tag{1}$$

For more details of the equations necessary to obtain the previous contributions, go to previous works.[55, 56] The five adjustable parameters for pure fluids required by this EoS are: the number of segments (m), the segment diameter (σ), the depth of pair potential energy (ε/k_B), the association energy of interaction (ε^{AB}/k_B), and the effective volume of interaction (κ^{AB}). To consider the hydrogen bonding interaction between molecules of the same type and different molecules, it is necessary to use an association scheme. The alcohols will be considered as self-associating with a 2B scheme, i.e., one positive site in hydrogen atom and one negative site in oxygen atom, while the DES is considered as pseudo-pure component with two association sites (2B scheme) to allow for self-association between the HBA and the HBD of the DES to form a hydrogen bond. Therefore, in the binary mixtures, the cross-association between DES and alcohol is considered, from the HBA and HBD interaction. On the other hand, for the binary mixtures, the following mixing rules are required:

$$\sigma_{ij} = \frac{1}{2}(\sigma_i + \sigma_j) \tag{2}$$

$$\varepsilon_{ij} = \sqrt{\varepsilon_i \varepsilon_j}(1 - k_{ij}) \tag{3}$$

$$\varepsilon^{A_iB_j} = \frac{1}{2}\left(\varepsilon^{A_iB_i} + \varepsilon^{A_jB_j}\right) \tag{4}$$

$$\kappa^{A_iB_j} = \sqrt{\kappa^{A_iB_i}\kappa^{A_jB_j}}\left[\frac{\sqrt{\sigma_i\sigma_j}}{(\sigma_i + \sigma_j)/2}\right]^3 \tag{5}$$

Therefore, k_{ij} is the binary interaction parameter and can be obtained by fitting experimental density data for binary mixtures.

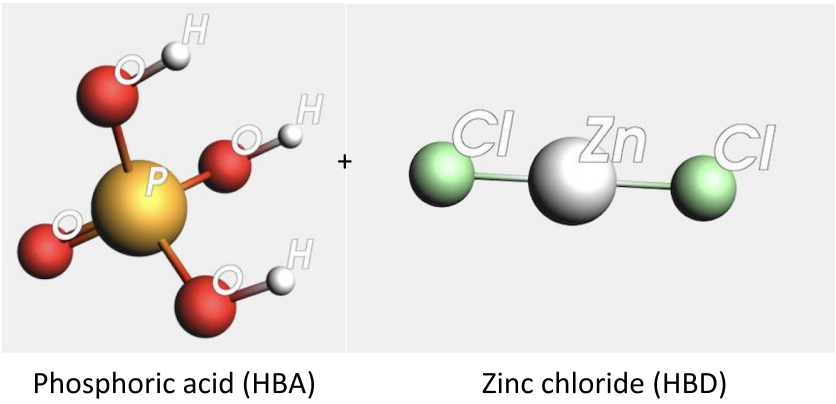

FIGURE 1 Structure of deep eutectic solvent (DES).

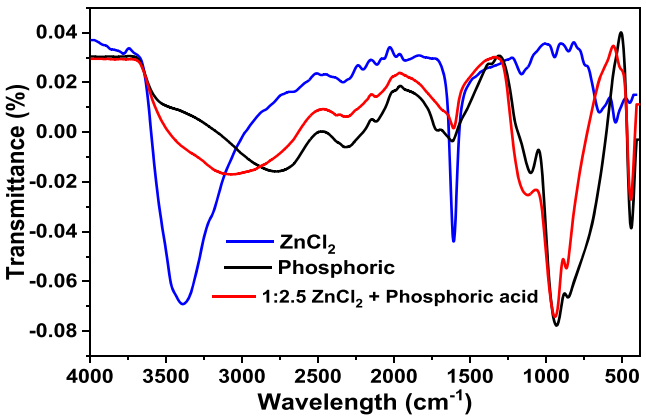

FIGURE 2 FTIR spectra for pure zinc chloride and phosphoric acid including [zinc chloride + phosphoric acid] 1:2.5 deep eutectic solvent.

3.2 | Speed of sound

Schaaff's collision factor theory (SCFT)[57] and Nomoto's relation (NR)[58] were used for modeling the speed of sound for binary mixtures.

From SCFT, the speed of sound is given by Equation (6):

$$u = \rho\, u_\infty (x_1 s_1 + x_2 s_2)(x_1 B_1 + x_2 B_2) \tag{6}$$

where ρ is the molar density of the mixture, which can be obtained from PC-SAFT EoS, $u_\infty = 1600$ m/s, s_i $(i = 1,2)$ is the space filling factor of component i in the mixture and can be compute using Equation (6), experimental speed of sound of the pure fluid, and molar density of the pure fluid obtained with PC-SAFT EoS. x_i $(i = 1,2)$ is the liquid mole fraction, and B_i $(i = 1,2)$ is the actual volume of the molecule per mole of component i, which is given by Equation (7):

$$B_i = N_A m_i \frac{\pi}{6} d_i^3 \tag{7}$$

with N_A, the Avogadro constant.

On the other hand, the speed of sound from NR is given by Equation (8):

$$u = \left(\frac{x_1 D_1 + x_2 D_2}{\frac{x_1}{\rho_1} + \frac{x_2}{\rho_2}} \right)^3, \; D_i = \frac{1}{\rho_i} u_i^{1/3} \tag{8}$$

where D_i, ρ_i, and u_i, stand the molar speed of sound, the molar density of the pure fluid obtained with PC-SAFT, and the experimental speed of sound for the pure fluid, respectively.

4 | RESULTS AND DISCUSSION

4.1 | Measured properties

The experimental values of the densities, and speed of sound of a binary mixture of ([$ZnCl_2$][phosphoric acid] 1:2.5 + methanol), ([$ZnCl_2$][phosphoric acid] 1:2.5 + ethanol) and ([$ZnCl_2$][phosphoric acid] 1:2.5 + propanol) at T = (293.15, 303.15, 308.15, and 313.15) K and at a pressure, $p = 1$ bar are presented. Excess molar volumes (V_m^E), isentropic compressibilities (κ_s), excess isentropic compressibilities ($\Delta\kappa_s$), and intermolecular free length (L_f) of the studied binary solutions were calculated from the experimental densities (ρ), speed of sound (u), using Equations (9)–(12), respectively.

$$V_m^E = \frac{x_1 M_1 - x_2 M_2}{\rho} - \frac{x_1 M_1}{\rho_1} - \frac{x_2 M_2}{\rho_2} \tag{9}$$

$$\kappa_s = \frac{1}{\rho u^2} \tag{10}$$

$$\Delta\kappa_s = \kappa_s - (x_1 K_1 + x_2 K_2) \tag{11}$$

where and x_2 are mole fractions, M_1 and M_2 are the molecular masses, ρ_1 and ρ_2 are the densities of pure

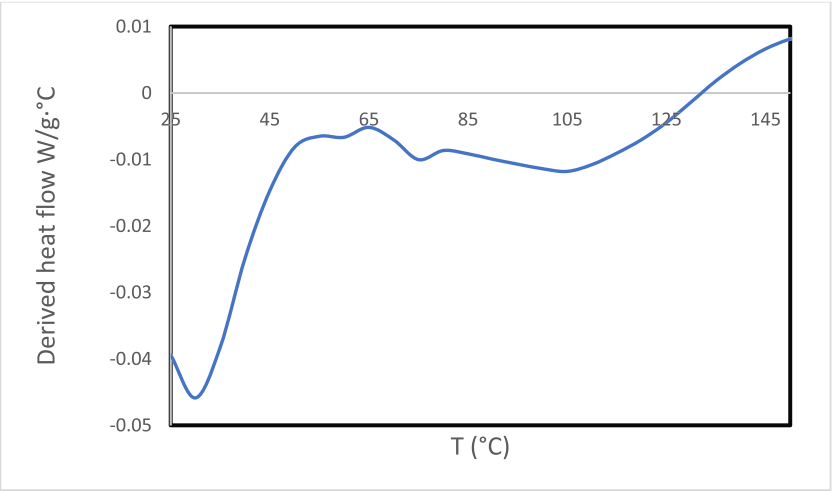

FIGURE 3 DSC spectra for the prepared deep eutectic solvent [zinc chloride + phosphoric acid] 1:2.5 M ratio.

components 1 and 2, respectively, where '1' refers to [$ZnCl_2$][phosphoric acid] 1:2.5 and '2' refers to methanol, ethanol, or propanol ρ, u, and K_s is the density speed of sound, and isentropic compressibilities of the mixtures, respectively. Equations (10) and (11) were used to calculate the isentropic compressibility and excess isentropic compressibilities for the mixtures. Intermolecular free length (L_f)were calculated using the below Equation (12)

$$L_f = K_j (K_s)^{\frac{1}{2}} \tag{12}$$

In the equation above, Jacobson's constant temperature dependent $(93.875 + .375\ T)10^{-8}$ is denoted by K_j and K_s denote the isentropic compressibility.

The ρ, u, κ_s, L_f, (Table 3) and V_m^E, $\Delta\kappa_s$ (Table S1) of the binary mixtures ([$ZnCl_2$][phosphoric acid] 1:2.5 + methanol), ([$ZnCl_2$][phosphoric acid] 1:2.5 + ethanol), ([$ZnCl_2$][phosphoric acid] 1:2.5 + propanol) at T = (293.15, 303.15, 308.15, and 313.15) K are presented.

4.1.1 | The influence of composition on density

The influence of composition on density is an important concept in understanding the physical properties of materials and is used in many scientific and engineering applications, such as in designing materials for specific purposes or in analyzing the properties of natural materials.[59,60]

In this study, the density of the solution is directly proportional to the mole fraction of the DES, meaning that as the concentration of the solvent increases, the density of the solution also increases as shown in Table 3 and Figure S2.[61] This is because the [$ZnCl_2$][phosphoric acid] 1:2.5 is usually the component with a higher molecular weight and density, and its presence in a larger quantity in the mixture results in a higher overall density.

On the other hand, the density of a binary mixture decreases as the temperature increases at all intervals.[62] This is because, at higher temperatures, the molecules in the mixture have higher kinetic energy, which causes them to move more rapidly and occupy a larger volume. As a result, the density of the mixture decreases.

Overall, the relationship between density, solvent concentration, and temperature in binary mixtures can be expressed by the following equation:

$$\text{Density} = f\,(\text{Solvent Concentration}, \text{Temperature})$$

where f is a function that relates the mixture's density to the solvent's concentration and the system's temperature.[63]

4.1.2 | The influence of temperature and composition on speed of sound

The speed of sound in a liquid or gas depends on various factors, including the density and compressibility of the medium.[64,65] It was noted that the speed of sound increases with an increase in the concentration of the [$ZnCl_2$][phosphoric acid] 1:2.5 DES (Table 3 and Figure S3). This is because the addition of DES molecules to a solution increases the density of the medium, making it more difficult for sound waves to propagate through it. As a result, the speed of sound increases.

However, the speed of sound in a [$ZnCl_2$][phosphoric acid] 1:2.5 DES decreases as the temperature increases. This is because the thermal motion of molecules increases with temperature, which causes the medium to become less dense and less compressible. As a result, it becomes easier for sound waves to propagate through the medium, and the speed of sound decreases.

It is worth noting that the effect of concentration on sound velocity may depend on the specific solvent and

TABLE 3 Densities, ρ, speed of sound, u, isentropic compressibilities and intermolecular free length, L_f, for the binary mixture {[$ZnCl_2$][phosphoric acid] 1:2.5 (x_1) + methanol, ethanol, or propanol (x_2)} at $T = (293.15, 303.15, 308.15, \text{and } 313.15)$ K and at .1 MPa.

x_1	$\rho/(\text{g}\cdot\text{cm}^{-3})$	$u/(\text{m}\cdot\text{s}^{-1})$	$\kappa_s/(\text{TPa}^{-1}) \cdot 10^{-2}$	L_f (nm) $\cdot 10^2$
{[$ZnCl_2$][phosphoric acid] 1:2.5 (x_1) + methanol (x_2)}				
$T = 293.15$				
.0000	.7916	1119.60	10.08	6.47
.1558	1.0390	1200.13	6.68	5.27
.2802	1.2200	1302.70	4.83	4.48
.4663	1.4600	1413.26	3.43	3.77
.6001	1.6072	1439.82	3.00	3.53
.7001	1.7012	1459.11	2.76	3.39
.7779	1.7690	1477.73	2.59	3.28
.8395	1.8200	1492.58	2.47	3.20
.8909	1.8587	1505.30	2.37	3.14
.9329	1.8880	1515.69	2.31	3.09
.9688	1.9141	1523.76	2.25	3.06
.9849	1.9274	1528.77	2.22	3.04
1.0000	1.9424	1537.77	2.18	3.01
$T = 303.15$				
.0000	.7822	1087.20	10.82	6.83
.1558	1.0300	1172.75	7.06	5.51
.2802	1.2110	1280.96	5.03	4.66
.4663	1.4516	1397.17	3.53	3.90
.6001	1.5985	1424.85	3.08	3.64
.7001	1.6937	1444.85	2.83	3.49
.7779	1.7628	1463.82	2.65	3.38
.8395	1.8142	1478.82	2.52	3.30
.8909	1.8528	1491.58	2.43	3.23
.9329	1.8827	1501.99	2.35	3.18
.9688	1.9090	1510.01	2.30	3.15
.9849	1.9223	1515.01	2.27	3.12
1.0000	1.9372	1520.24	2.23	3.10
$T = 308.15$				
.0000	.7776	1071.07	11.21	7.01
.1558	1.0254	1159.10	7.26	5.64
.2802	1.2070	1269.96	5.14	4.75
.4663	1.4473	1388.81	3.58	3.96
.6001	1.5937	1417.46	3.12	3.70
.7001	1.6890	1437.87	2.86	3.54
.7779	1.7580	1457.00	2.68	3.43
.8395	1.8093	1472.08	2.55	3.34
.8909	1.8479	1484.87	2.45	3.28
.9329	1.8777	1495.27	2.38	3.23
.9688	1.9039	1503.29	2.32	3.19
.9849	1.9172	1508.28	2.29	3.17
1.0000	1.9321	1513.47	2.26	3.15

TABLE 3 (Continued)

x_1	$\rho/(g \cdot cm^{-3})$	$u/(m \cdot s^{-1})$	$\kappa_s/(TPa^{-1}) \cdot 10^{-2}$	L_f (nm) $\cdot 10^2$
$T = 313.15$ K				
.0000	.7727	1055.00	11.63	7.21
.1558	1.0208	1145.58	7.46	5.77
.2802	1.2020	1259.18	5.25	4.84
.4663	1.4424	1380.77	3.64	4.03
.6001	1.5890	1410.20	3.16	3.76
.7001	1.6843	1430.97	2.90	3.60
.7779	1.7532	1450.28	2.71	3.48
.8395	1.8044	1465.44	2.58	3.39
.8909	1.8430	1478.26	2.48	3.33
.9329	1.8727	1488.65	2.41	3.28
.9688	1.8989	1496.67	2.35	3.24
.9849	1.9122	1501.66	2.32	3.22
1.0000	1.9271	1506.81	2.29	3.19
{[$ZnCl_2$][phosphoric acid] 1:2.5 (x_1) + ethanol (x_2)}				
$T = 293.15$ K				
.0000	.7896	1160.37	9.41	6.25
.1559	.9801	1235.88	6.68	5.27
.2810	1.1316	1322.11	5.06	4.58
.4904	1.3818	1408.50	3.65	3.89
.6000	1.5073	1418.87	3.30	3.70
.6999	1.6185	1443.33	2.97	3.51
.7771	1.7035	1464.41	2.74	3.37
.8397	1.7710	1481.15	2.57	3.27
.8906	1.8238	1496.19	2.45	3.19
.9331	1.8660	1509.52	2.35	3.13
.9690	1.9021	1521.68	2.27	3.07
.9845	1.9205	1526.43	2.23	3.05
1.0000	1.9424	1537.77	2.18	3.01
$T = 303.15$ K				
.0000	.7810	1126.91	10.08	6.59
.1559	.9713	1201.47	6.74	5.39
.2810	1.1230	1295.41	5.09	4.68
.4904	1.3732	1389.45	3.67	3.98
.6000	1.4985	1401.44	3.31	3.78
.6999	1.6114	1427.67	2.98	3.58
.7771	1.6971	1448.72	2.75	3.44
.8397	1.7650	1467.00	2.58	3.34
.8906	1.8179	1482.46	2.46	3.25
.9331	1.8605	1495.77	2.36	3.19
.9690	1.8973	1507.95	2.28	3.13
.9845	1.9155	1512.69	2.24	3.11
1.0000	1.9372	1520.24	2.23	3.10

(Continues)

TABLE 3 (Continued)

x_1	$\rho/(g \cdot cm^{-3})$	$u/(m \cdot s^{-1})$	$\kappa_s/(TPa^{-1}) \cdot 10^{-2}$	L_f (nm) $\cdot 10^2$
$T = 308.15$ K				
.0000	.7723	1109.94	10.51	6.79
.1559	.9629	1220.15	6.98	5.53
.2810	1.1140	1295.98	5.34	4.84
.4904	1.3639	1379.43	3.85	4.11
.6000	1.4902	1392.74	3.46	3.90
.6999	1.6041	1419.89	3.09	3.68
.7771	1.6896	1441.45	2.85	3.53
.8397	1.7586	1460.02	2.67	3.42
.8906	1.8119	1475.69	2.53	3.33
.9331	1.8553	1489.03	2.43	3.27
.9690	1.8927	1501.23	2.34	3.21
.9845	1.9111	1505.97	2.31	3.18
1.0000	1.9321	1513.47	2.26	3.15
$T = 313.15$ K				
.0000	.7701	1093.40	10.86	6.96
.1559	.9602	1201.91	7.21	5.67
.2810	1.1118	1279.60	5.49	4.95
.4904	1.3605	1369.43	3.92	4.18
.6000	1.4869	1384.12	3.51	3.96
.6999	1.5999	1412.17	3.13	3.74
.7771	1.6858	1434.26	2.88	3.59
.8397	1.7549	1453.12	2.70	3.47
.8906	1.8082	1468.98	2.56	3.38
.9331	1.8514	1482.37	2.46	3.31
.9690	1.8889	1494.59	2.37	3.25
.9845	1.9063	1499.34	2.33	3.23
1.0000	1.9271	1506.81	2.29	3.19
{[$ZnCl_2$][phosphoric acid] 1:2.5 (x_1) + propanol (x_2)}				
$T = 293.15$ K				
.0000	.8036	1222.69	8.32	5.88
.1558	.9560	1263.35	6.55	5.22
.2807	1.0860	1295.98	5.48	4.77
.4668	1.2915	1342.65	4.30	4.22
.6021	1.4471	1380.63	3.63	3.88
.6998	1.5624	1411.58	3.21	3.65
.7777	1.6586	1439.81	2.91	3.48
.8395	1.7377	1464.18	2.68	3.34
.8903	1.8012	1485.18	2.52	3.23
.9333	1.8530	1503.67	2.39	3.15
.9687	1.8931	1521.20	2.28	3.08
.9851	1.9162	1523.81	2.25	3.06
1.0000	1.9424	1537.77	2.18	3.01

TABLE 3 (Continued)

x_1	$\rho/(\mathrm{g{\cdot}cm^{-3}})$	$u/(\mathrm{m{\cdot}s^{-1}})$	$\kappa_s/(\mathrm{TPa^{-1}}) \cdot 10^{-2}$	L_f (nm) $\cdot 10^2$
$T = 303.15$ K				
.0000	.7956	1188.88	8.89	6.19
.1558	.9486	1232.26	6.94	5.47
.2807	1.0778	1267.99	5.77	4.99
.4668	1.2840	1319.67	4.47	4.39
.6021	1.4396	1361.01	3.75	4.02
.6998	1.5554	1394.06	3.31	3.78
.7777	1.6522	1423.86	2.99	3.59
.8395	1.7314	1449.25	2.75	3.44
.8903	1.7956	1470.88	2.57	3.33
.9333	1.8480	1489.71	2.44	3.24
.9687	1.8884	1506.58	2.33	3.17
.9851	1.9113	1509.90	2.29	3.14
1.0000	1.9372	1520.24	2.23	3.10
$T = 308.15$ K				
.0000	.7916	1171.93	9.20	6.35
.1558	.9454	1216.62	7.15	5.60
.2807	1.0743	1253.92	5.92	5.10
.4668	1.2797	1308.15	4.57	4.48
.6021	1.4355	1351.22	3.82	4.09
.6998	1.5510	1385.39	3.36	3.84
.7777	1.6478	1415.97	3.03	3.64
.8395	1.7275	1441.89	2.78	3.49
.8903	1.7913	1463.84	2.61	3.38
.9333	1.8441	1482.87	2.47	3.29
.9687	1.8841	1499.28	2.36	3.22
.9851	1.9072	1503.17	2.32	3.19
1.0000	1.9321	1513.47	2.26	3.15
$T = 313.15$ K				
.0000	.7875	1155.23	9.52	6.52
.1558	.9422	1201.06	7.36	5.73
.2807	1.0709	1239.92	6.07	5.21
.4668	1.2761	1296.77	4.66	4.56
.6021	1.4312	1341.50	3.88	4.16
.6998	1.5468	1376.80	3.41	3.90
.7777	1.6441	1408.16	3.07	3.70
.8395	1.7232	1434.61	2.82	3.55
.8903	1.7869	1456.88	2.64	3.43
.9333	1.8398	1476.11	2.49	3.34
.9687	1.8798	1491.97	2.39	3.27
.9851	1.9028	1496.62	2.35	3.24
1.0000	1.9271	1506.81	2.29	3.19

Note: Standard uncertainties u are $u(T) = .02$ K, $u(p) = .04$ MPa, and the combined expanded uncertainties Uc in mole fraction, density, and speed of sound were $Uc(x) = .0006$, $Uc(\rho) = .0009$ g·cm^{-3}, $Uc(\underline{u}) = 2.63$ m·s^{-1}, respectively (.95 level of confidence).

solute being used, as well as the temperature and pressure conditions.

4.2 | Calculated properties

4.2.1 | Excess molar volumes

Excess molar volume (V_m^E) is a thermodynamic property that describes the deviation of the mixture's volume from an ideal mixture's volume.[66,67] It is defined as the difference between the actual molar volume of the mixture and the molar volume of an ideal mixture. Tables S1, as well as Figure 4, provide a summary of the calculated results.

Over the entire mole fraction range, at all investigated temperatures, and for all investigated binary systems, both negative and positive values for the calculated excess molar volume were observed.[68,69] Positive excess molar volume values are found at higher [$ZnCl_2$][phosphoric acid] 1:2.5 DES mole fractions. The magnitude and sign of the excess molar volume values are influenced by several factors, including volume expansion and contraction effects, as well as other factors such as the chemical nature and concentration of the components, the temperature, and the pressure. Volume expansion occurs when the intermolecular forces between the two components are weaker than those within the pure components, leading to an increase in the overall volume of the mixture. In contrast, volume contraction occurs when the intermolecular forces between the two components are stronger than those within the pure components, leading to a decrease in the overall volume of the mixture.

When a polar solvent like [$ZnCl_2$][phosphoric acid] 1:2.5 DES and alcohol are mixed, they can interact via dipole–dipole interactions between their polar molecules. The polar molecules of the two solvents can attract each other, causing a decrease in the volume of the mixture. This effect can contribute to the decreased volume observed in the excess molar volumes of DES-alcohol mixtures.

In the case of phosphoric acid (hydrogen bond donor from DES) and alcohols (methanol, ethanol, and propanol), the negative excess molar volume may be due to the formation of hydrogen bonds between the acid and alcohol molecules. Phosphoric acid has three hydroxyl groups ($^-$OH) and can form hydrogen bonds with alcohol molecules that also have hydroxyl groups. The hydrogen bond formation between the oxygen atom of the (H_3PO_4) group of phosphoric acid and the hydrogen atom of the hydroxyl group of alcohol molecules leads to a more compact arrangement of molecules in the mixture, resulting in a negative excess molar volume.

It is worth noting that not all negative V_m^E can be attributed to hydrogen bonding between the components. Other factors such as changes in the packing efficiency or changes in the attractive forces between the molecules can also contribute to negative excess molar volumes.

On the other hand, V_m^E indicates that the volume of the mixture is greater than the sum of the volumes of its components, suggesting that there is a certain degree of repulsive interaction between the molecules in the mixture, such as steric hindrance or electrostatic repulsion.[70,71] When the excess molar volume is positive, it means that the mixture's actual molar volume is greater than expected based on ideal solution behavior.[72] This indicates that the mixing process results in an overall expansion of the mixture. There are several factors that can contribute to a positive excess molar volume, including differences in molecular size, shape, and polarity between the two substances being mixed. In general, substances that are more dissimilar tend to have larger positive excess molar volumes.

The alkyl chain length of the alcohol can affect the polarity and hydrogen bonding capabilities of the molecule, which in turn can affect the interactions between the alcohol and the deep eutectic solvent. In this case, increasing the alkyl chain length of the alcohol is leading to a decrease in the solubility of the alcohol in the deep eutectic solvent, which results in a decrease in the excess molar volume.

4.2.2 | Isentropic compressibility

Isentropic compressibility is a measure of the degree to which a substance can be compressed under adiabatic (no heat exchange) conditions.[73] Tables 3 as well as Figure S4 presents the isentropic compressibility, κ_s, results for the binary systems of [$ZnCl_2$][phosphoric acid] 1:2.5 in methanol, ethanol, or propanol at different temperatures. Figure S4 plots the results against the mole fractions of [$ZnCl_2$][phosphoric acid] 1:2.5 at all temperatures. The Newton–Laplace method was used to compute the isentropic compressibility (κ_s) (Equation (10)).

Isentropic compressibility values increase with increasing temperature and solvent composition, [$ZnCl_2$][phosphoric acid] 1:2.5, indicating greater compressibility of DES in solutions.[74] Isentropic compressibility is positive at all temperatures due to stronger interactions between methanol, ethanol, or propanol, and solvent molecules [$ZnCl_2$][phosphoric acid] 1:2.5, making the solution more compressible than pure solvents. This is also an indication of the [$ZnCl_2$][phosphoric acid] 1:2.5 molecule's or ions' closest approach with stronger interactions that increase the compressibility of the binary mixtures.[75] Positive isentropic compressibility means that the substance can be compressed without an increase in its internal energy or temperature. In other words, a substance

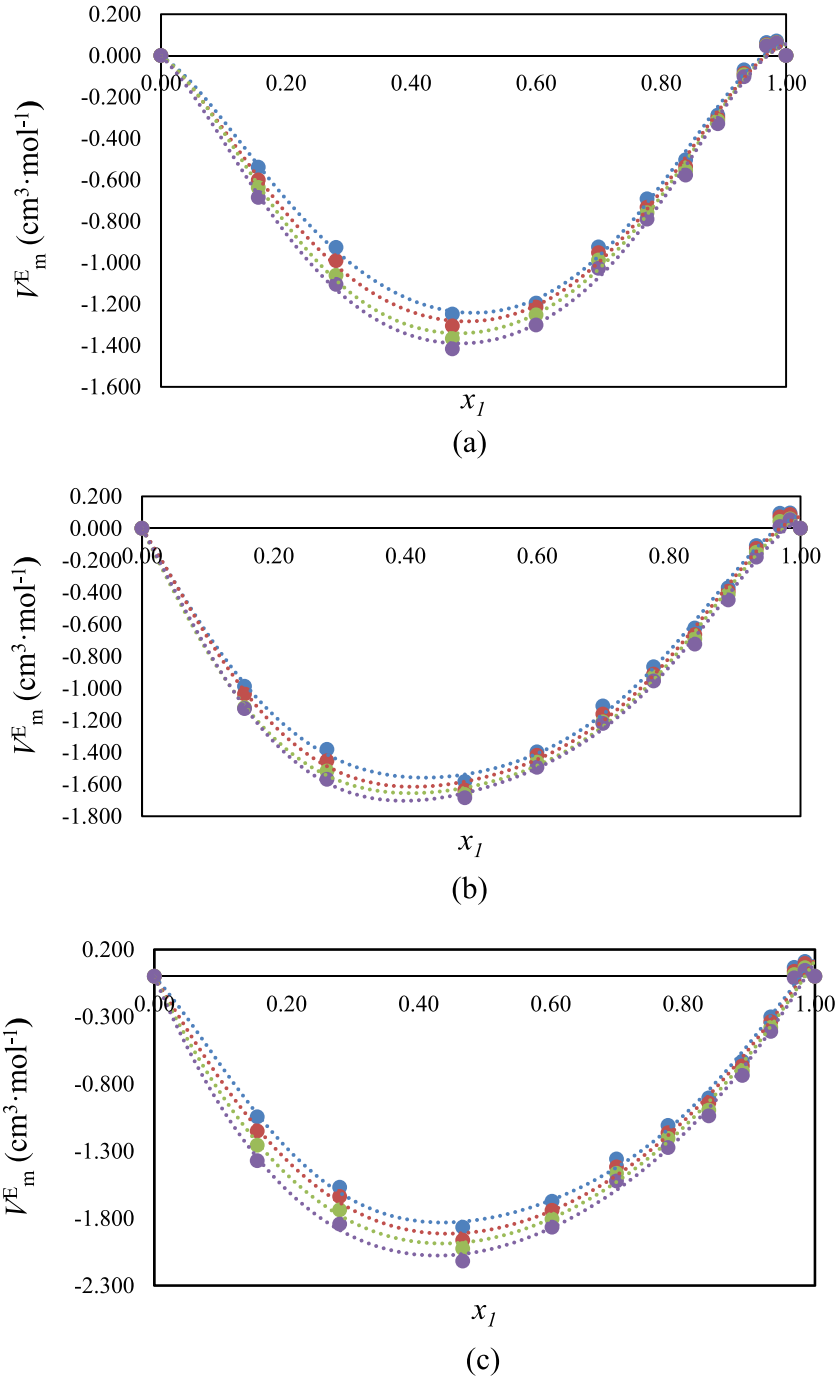

FIGURE 4 Calculated excess molar volumes, V_m^E, for the binary mixtures of {[$ZnCl_2$] [phosphoric acid] 1:25 (x_1) + methanol (a), ethanol (b), and propanol (c)} at 293.15 K (blue), 303.15 K (red), 308.15 K (green), 313.15 K (purple).

with a positive isentropic compressibility will decrease in volume when subjected to an increase in pressure, without a corresponding increase in its temperature.

4.2.3 | Excess isentropic compressibility

The $\Delta\kappa_s$ is a measure of the deviation from ideal behavior in a mixture of two or more components. It is defined as the difference between the isentropic compressibility of the mixture and the isentropic compressibility that would be expected if the mixture behaved ideally.[76,77] A negative excess compressibility values were noted for all calculated binary mixtures (Table S1 and Figure 5). It indicates that the mixture is less compressible than expected based on the ideal behavior. This can happen if the interactions between the molecules of the components in the mixture are attractive, causing them to pack more closely together and resist compression more than expected. It can also occur if the mixture contains components with very different sizes or shapes, which can hinder their ability to move and pack together efficiently.

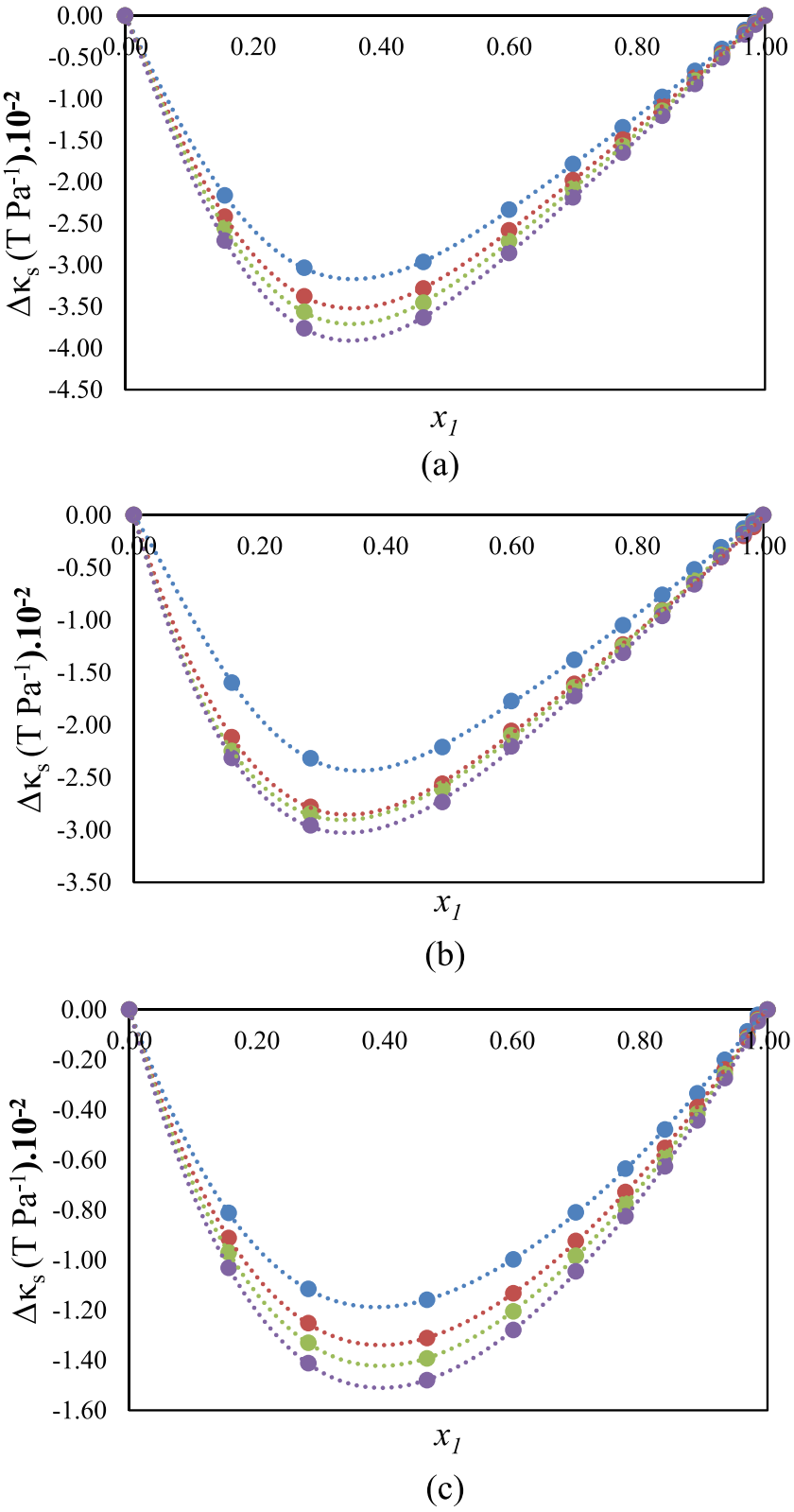

FIGURE 5 Calculated excess isentropic compressibilities, $\Delta\kappa_s$, of the binary mixtures of {[$ZnCl_2$][phosphoric acid] 1:2.5 (x_1) + methanol (a), ethanol (b), and propanol (c)} at 293.15 K (blue), 303.15 K (red), 308.15 K (green), and 313.15 K (purple).

Negative excess isentropic compressibility can be important in understanding the behavior of mixtures in various industrial and scientific applications, such as in chemical processing, material science, and geology.

The addition of a longer alkyl chain alcohol to the deep eutectic solvent may increase the negative excess isentropic compressibility, as the longer chain may introduce more flexibility to the solvent molecules and increase the free volume. However, this effect may be counteracted by other factors, such as the formation of hydrogen bonds between the alcohol and the DES, which can reduce the free volume.

4.2.4 | Intermolecular free length

The intermolecular free length of a binary mixture is a measure of the average distance between molecule in the mixture.[78] It is known as the mean free path or the average distance between collisions. It can be calculated from the speed of sound in the mixture, which is related to the density and compressibility of the mixture. In a binary mixture, the intermolecular free length can be used to determine the properties that exist based on the attractive and repulsive forces as well as a simple linear correlation with the mole fraction of the deep eutectic solvent between the different types of molecules.

The use of intermolecular free length and its correlation with the mole fraction of the deep eutectic solvent can provide valuable information for the design and optimization of binary mixtures with both attractive and repulsive forces. Because of the increase in [$ZnCl_2$][phosphoric acid] 1:2.5 DES content, intermolecular forces between the molecules in a mixture are attractive, and molecules tend to come closer together, resulting in a smaller intermolecular free length (Table 3 and Figure 6). As the temperature increase, speed of sound in [$ZnCl_2$][phosphoric acid] 1:2.5 DES also increase. This is because the speed of sound is related to the average kinetic energy of the particles in the substances, which increases the temperature. However, the compressibility of a substance generally decreases as the temperature the temperature increases. This is because, at higher temperatures, the particles have more kinetic energy and are more likely to overcome the attractive forces between them, making the substance less compressible. Therefore, as the compressibility of a [$ZnCl_2$][phosphoric acid] 1:2.5 DES decreases with increasing temperature, the decrease intermolecular free length was observed in Table 3.

4.2.5 | Excess thermal expansibilities

Thermal expansivities, α, were calculated from the density and V^E results, to allow better understanding of change in the solution structure during blending. Thermal expansion coefficients for pure components and compositions for the binary mixture, respectively are expressed from Equations (13) and (14), respectively,

$$\alpha_i = \left(1/V_i^0\right)\left(\partial V_i^0/\partial T\right)_P \tag{13}$$

$$\alpha = (1/V)\left[\left(\partial V_m^E/\partial T\right)_{P,x} + \sum_{i=1}^{i=2} \alpha_i x_i V_i^0\right] \tag{14}$$

where V_i^0 and V is the molar volume of pure fluid and molar volume of the mixture, respectively.

Excess thermal expansibilities, α^E, were calculated from Equation (15):

$$\alpha^E = \alpha - \sum_{i=1}^{i=2} \emptyset_i \alpha_i \tag{15}$$

where $\emptyset_i$ is the volume fraction of the pure component i, defined as follows:

$$\emptyset_i = \left(x_i V_i^0 / \sum_i x_i V_i^0\right) \tag{16}$$

Table 4 show the values of the thermal expansibilities and excess thermal expansivity at four temperatures. The coefficients of thermal expansion for all the binary mixtures decrease with increasing DES mole fraction. According to Table 4, the values of excess thermal expansion coefficients are positive for the majority of the DES mole fraction, except for mole fractions very close to pure DES. The same results can be observed in Figure 7.

4.3 | Correlations

4.3.1 | Redlich–Kister correlation

The Redlich–Kister fitting parameters were calculated from Equation (17):

$$Z = x_1 x_2 \overset{i=0}{\underset{N}{\Sigma}} A_i (2x-1)^i, \tag{17}$$

where Z is the V_m^E or $\Delta\kappa_s$; x_1 is the mole fraction of the [$ZnCl_2$][phosphoric acid] 1:2.5; x_2 is the mole fraction of methanol, ethanol, and propanol; N is the degree of the polynomial expansion; and A_i is the Redlich–Kister parameters obtained for the system.

The root-mean-square deviation was calculated from Equation (18)

$$\sigma = \left(\frac{\sum_i^M \sum \left(Zcal_{exp}\right)()^{1/2}}{M-k}\right) \tag{18}$$

where Z_{exp}, Z_{cal}, are the values of the experimental and computed V_m^E or $\Delta\kappa_s$ and M is the number of experimental data points and k is the number of coefficients used in the Redlich–Kister correlation, respectively.

The Redlich–Kister parameters and the root mean square deviation for all binary systems are given in Table 5. The Redlich–Kister fitting smoothing polynomial was used to obtain the fitting parameters of the binary systems together with the standard deviations.[35,79] The Redlich–Kister smoothing equation was used successfully for the correlation of V_m^E and $\Delta\kappa_s$ data.

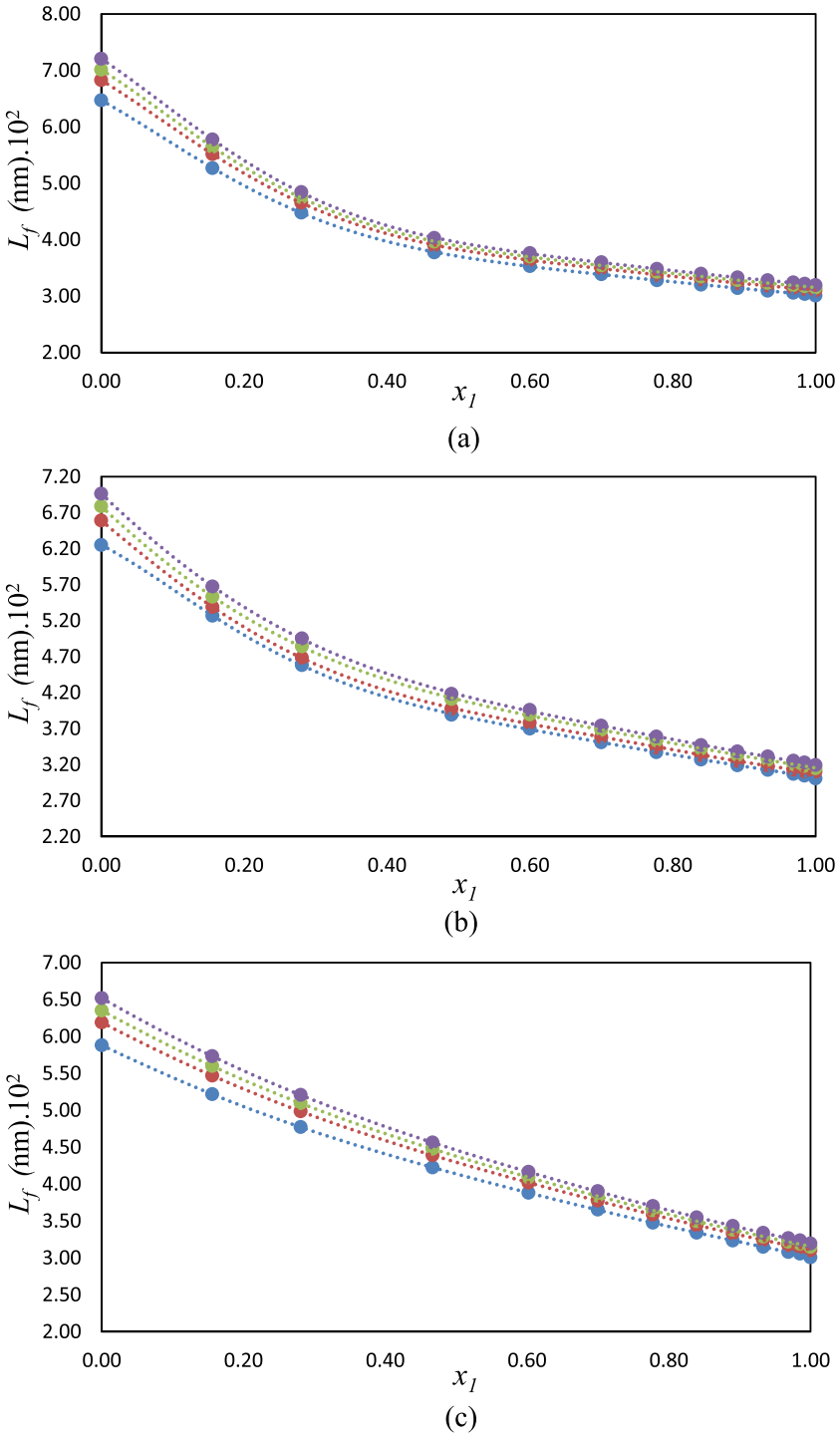

FIGURE 6 Plot of intermolecular free length L_f, of the binary mixtures of {[$ZnCl_2$] [phosphoric acid] 1:2.5 (x_1) + methanol (a), ethanol (b), and propanol (c)} at $T = (293.15, 303.15, 308.15, \text{and } 313.15)$ K}.

4.4 | Results for density and speed of sound

The parameters for the alcohols required in PC-SAFT were obtained from the literature.[56] In the case of DES, considered as a pseudo-pure fluid, the parameters were adjusted only with experimental density data using objective function given by Equation (19):

$$FO = \sum_{i=1}^{n_p} \left(\frac{\rho_i^{calc.} - \rho_i^{exp.}}{\rho_i^{exp.}} \right)^2 \quad (19)$$

where n_p is the number of experimental points, ρ is the density, *calc.* is calculated using PC-SAFT EoS, and *exp.* is experimental. On the other hand, the absolute average deviation was calculated as Equation (20):

TABLE 4 Isobaric thermal expansion coefficient and excess thermal expansion coefficient for the binary mixture {[$ZnCl_2$][phosphoric acid] 1:2.5 (x_1) + methanol, ethanol, or propanol (x_2)} at T = (293.15, 303.15, 308.15, and 313.15) K and at .1 MPa.

x_1	α /(K^{-1})	α^E /(K^{-1})
{[$ZnCl_2$][phosphoric acid] 1:2.5 (x_1) + methanol (x_2)}		
T = 293.15 K		
.0000	1.996	0
.1558	1.865	.023
.2802	1.767	.036
.4663	1.623	.042
.6001	1.521	.036
.7001	1.443	.026
.7779	1.386	.018
.8395	1.343	.013
.8909	1.306	.007
.9329	1.277	.002
.9688	1.254	−.001
.9849	1.245	−.002
1.0000	1.238	0
T = 303.15 K		
.0000	2.020	0
.1558	1.889	.026
.2802	1.788	.039
.4663	1.640	.044
.6001	1.533	.037
.7001	1.453	.027
.7779	1.395	.019
.8395	1.350	.013
.8909	1.312	.007
.9329	1.282	.002
.9688	1.258	−.001
.9849	1.249	−.001
1.0000	1.241	0
T = 308.15 K		
.0000	2.032	0
.1558	1.901	.028
.2802	1.800	.042
.4663	1.650	.047
.6001	1.541	.038
.7001	1.460	.028
.7779	1.401	.020
.8395	1.355	.014
.8909	1.317	.008
.9329	1.286	.002
.9688	1.262	−.001
.9849	1.252	−.001
1.0000	1.245	0
T = 313.15 K		
.0000	2.045	0
.1558	1.914	.030
.2802	1.812	.044
.4663	1.660	.048
.6001	1.549	.040
.7001	1.467	.029
.7779	1.407	.021
.8395	1.360	.014
.8909	1.322	.008
.9329	1.290	.002
.9688	1.265	−.001
.9849	1.255	−.001
1.0000	1.248	0
{[$ZnCl_2$][phosphoric acid] 1:2.5 (x_1) + ethanol (x_2)}		
T = 293.15 K		
.0000	4.541	0
.1559	4.113	.070
.2810	3.729	.089
.4904	3.038	.084
.6000	2.656	.065
.6999	2.302	.045
.7771	2.028	.031
.8397	1.805	.020
.8906	1.623	.011
.9331	1.470	.003
.9690	1.342	−.002
.9845	1.289	−.002
1.0000	1.238	0
T = 303.15 K		
.0000	4.591	0
.1559	4.163	.074
.2810	3.776	.095
.4904	3.076	.087
.6000	2.686	.066
.6999	2.328	.047
.7771	2.049	.033
.8397	1.822	.021
.8906	1.635	.011
.9331	1.479	.003
.9690	1.348	−.002
.9845	1.294	−.002
1.0000	1.241	0

(Continues)

(Continues)

TABLE 4 (Continued)

x_1	α /(K^{-1})	α^E /(K^{-1})
T = 308.15 K		
.0000	4.643	0
.1559	4.217	.080
.2810	3.825	.099
.4904	3.114	.089
.6000	2.719	.069
.6999	2.355	.050
.7771	2.069	.034
.8397	1.838	.022
.8906	1.647	.012
.9331	1.488	.004
.9690	1.355	−.001
.9845	1.299	−.001
1.0000	1.245	0
T = 313.15 K		
.0000	4.656	0
.1559	4.230	.080
.2810	3.839	.102
.4904	3.123	.090
.6000	2.728	.070
.6999	2.362	.050
.7771	2.076	.035
.8397	1.844	.023
.8906	1.653	.013
.9331	1.493	.005
.9690	1.359	0
.9845	1.303	−.001
1.0000	1.248	0
{[$ZnCl_2$][phosphoric acid] 1:2.5 (x_1) + propanol (x_2)}		
T = 293.15 K		
.0000	5.706	0
.1558	5.239	.076
.2807	4.803	.109
.4668	4.050	.114
.6021	3.421	.090
.6998	2.928	.064
.7777	2.517	.046
.8395	2.179	.033
.8903	1.889	.020
.9333	1.635	.008
.9687	1.421	−.002
.9851	1.324	−.003
1.0000	1.238	0
T = 303.15 K		
.0000	5.764	0
.1558	5.302	.084
.2807	4.859	.113
.4668	4.100	.121
.6021	3.462	.094
.6998	2.962	.068
.7777	2.545	.049
.8395	2.200	.035
.8903	1.905	.022
.9333	1.647	.010
.9687	1.429	−.001
.9851	1.329	−.002
1.0000	1.241	0
T = 308.15 K		
.0000	5.793	0
.1558	5.336	.092
.2807	4.891	.120
.4668	4.126	.125
.6021	3.484	.098
.6998	2.980	.070
.7777	2.559	.051
.8395	2.213	.037
.8903	1.915	.023
.9333	1.655	.011
.9687	1.434	0
.9851	1.334	−.002
1.0000	1.245	0
T = 313.15 K		
.0000	5.823	0
.1558	5.373	.100
.2807	4.925	.128
.4668	4.154	.131
.6021	3.506	.101
.6998	2.999	.073
.7777	2.575	.054
.8395	2.225	.054
.8903	1.924	.024
.9333	1.662	.012
.9687	1.439	0
.9851	1.338	−.001
1.0000	1.248	0

Note: Standard uncertainties u are $u(T)$ = .02 K, $u(p)$ = .04 MPa, and the combined expanded uncertainties Uc in mole fraction, density, and speed of sound were $Uc(x)$ = .0006, $Uc(\rho)$ = .0009 g·cm^{-3}, $Uc(\underline{u})$ = 2.63 m·s^{-1}, respectively (.95 level of confidence).

(Continues)

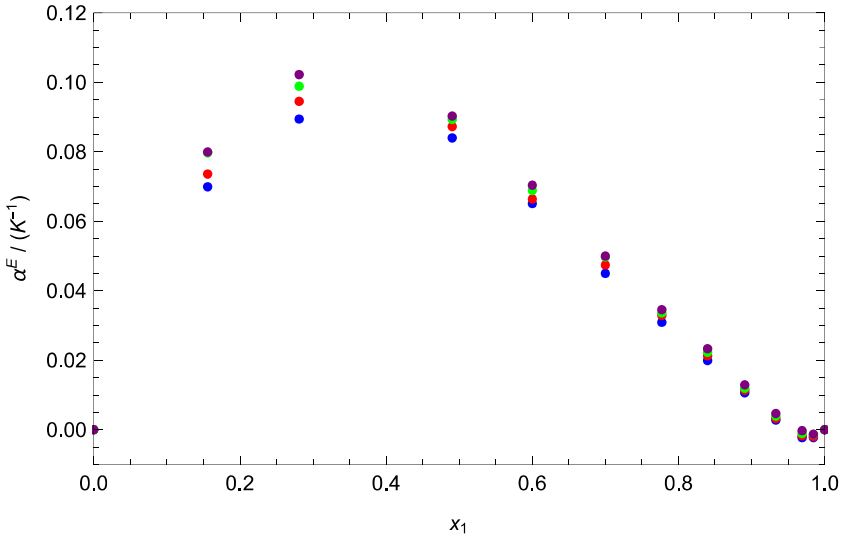

FIGURE 7 Plot of excess thermal expansion coefficients of {[$ZnCl_2$][phosphoric acid] 1:2.5 (x_1) + ethanol (x_2)} at different temperatures as a function of the composition expressed in the mole fraction of [$ZnCl_2$][phosphoric acid] 1:2.5 at 293.15 K (blue), 303.15 K (red), 308.15 K (green), and 313.15 K (purple).

$$\%AAD\varphi = \frac{100}{n_p}\sum_{i=1}^{n}\frac{\left|\varphi_i^{exp.} - \varphi_i^{calc.}\right|}{\varphi_i^{exp.}} \quad (20)$$

where φ is density or speed of sound. The parameters obtained in this work were $m = 2.100$, $\sigma = 3.5436$ Å, $\frac{\varepsilon}{k_B} = 772.4355$ K, $\kappa^{AB} = .003297$, and $\frac{\varepsilon^{AB}}{k_B} = 4276.8451$ K. The absolute average deviation in density was .05%.

The values of k_{ij} are positive for all the mixtures, and they are published in Table 6. Also, the deviation in density and speed of sound using SCFT and NR are available in Table 6. According to these results, PC-SAFT correlates the experimental density with the mole fraction with an overall deviation of .27%. In the case of the speed of sound, both equations correctly predict the experimental data, however for DES + 1-propanol mixture, NR (deviation = .32%), despite its simplicity, presents a lower deviation compared to SCFT (deviation = 1.99%). Finally, some graphic results are illustrated in Figures 8 and 9. According to Figure 8, the results with $k_{ij} = .3521$ for DES + methanol mixture, allow good results in the density correlation. From Figure 6, the best experimental speed of sound correlation for the DES + ethanol mixture was obtained with PC-SAFT EoS + SCFT. Recently, few studies have been reported for the simulation of DESs with volatile organic solvents at different temperatures. The structural orientation was studies with the selected volatile organic solvents and the results revealed high solubility at high molar ratio and this impact has been observed in our studies.[31,32]

4.5 | Sigma profiles and surface charges

The intermolecular interactions were further studied between the chemical species σ-profiles and sigma potentials of the DES with different solutes and are depicted in Figures 10 and 11, respectively. Sigma profiles can deliver crucial information on the hydrophilicity as well as the tendency of a compound in hydrogen bond donor and acceptor properties. As observed in Figure 10, each produced sigma profile exhibits three distinguished areas. The left-hand side area (<−.01 e/Å^2) is known as hydrogen bond (H-bond) donor and the regions with $\sigma >$ .01 e/Å^2 and $-.01 < \sigma <$ .01 e/Å2 are hydrogen bond acceptors or and non-polar regions, respectively. It is observed in Figure 10, that the surface charge density of phosphoric acid is dominated by the three distinctive regions: purple regions of non-polar alkyl chain, blue region of the H-bond acceptor region, and the red regions of the oxygen lone pairs, which are H-bond acceptors. Hence, phosphoric acid has shown three major peaks in H-bond acceptor, H-bond donor and non-polar regions as depicted in Figure 10. The addition of Methanol Ethanol and Propanol to the system results in the association of DES molecules to this chemical species based on their peaks in the abovementioned regions in Figure 10. For example, in the case of [$ZnCl_2$] the dominant peak represented in Figure 10 shows the non-polar surface area, which is a suitable partner surface for non-polar segments of different solutes and based on the length of the alkyl chain of different solutes it pairs more readily with propanol since it has shown the biggest peak in non-polar region. This confirms the results obtained in

TABLE 5 Redlich–Kister fitting parameters and root-mean-square deviation, σ, for the binary mixtures at $T = (293.15, 303.15, 308.15,$ and $313.15)$ K and at .1 MPa.

	A_i	293.15 K	303.15 K	308.15 K	313.15 K
{$ZnCl_2$][phosphoric acid] (x_1) + methanol (x_2)}					
$V_m^E/(cm^3 \cdot mol^{-1})$	A_0	−5.07206	−5.26356	−5.47790	−5.67405
	A_1	1.11783	1.57197	1.86950	1.85065
	A_2	3.31712	3.18079	2.85763	2.91990
	A_3	−7.85922	−9.40623	−9.82714	−9.54857
	A_4	−1.50922	−2.02911	−1.34595	−1.78171
	A_5	13.45640	15.3887	15.33090	15.57230
	σ	.04	.03	.03	.03
$\Delta\kappa_s/(TPa^{-1})$	A_0	−1132.500	−1254.040	−1318.250	−1386.930
	A_1	858.914	953.387	1007.220	1063.230
	A_2	−224.958	−279.539	−315.135	−346.553
	A_3	−525.784	−523.722	−530.085	−535.836
	A_4	240.408	281.329	319.688	340.506
	A_5	264.726	198.853	178.180	171.008
	σ	.30	.20	.21	.21
{$ZnCl_2$][phosphoric acid] (x_1) + ethanol (x_2)}					
$V_m^E/(cm^3 \cdot mol^{-1})$	A_0	−6.37255	−6.54092	−6.65878	−6.74921
	A_1	3.62630	3.85315	3.45799	3.63169
	A_2	2.29619	1.42293	.67025	.02265
	A_3	−14.29770	−14.46340	−10.92830	−10.54310
	A_4	−3.47987	−2.38689	−1.95530	−.72741
	A_5	23.50000	23.03660	18.92860	16.74900
	σ	.04	.03	.03	.03
$\Delta\kappa_s/(TPa^{-1})$	A_0	−869.944	−967.325	−1026.040	−1075.680
	A_1	689.901	758.244	788.543	815.719
	A_2	−179.625	−222.794	−277.463	−260.598
	A_3	−637.011	−672.840	−346.946	−392.202
	A_4	282.290	432.633	−165.468	−171.300
	A_5	361.356	215.931	541.947	568.046
	σ	.75	.84	.97	.98
{$ZnCl_2$][phosphoric acid] (x_1) + propanol (x_2)}					
$V_m^E/(cm^3 \cdot mol^{-1})$	A_0	−7.44748	−7.81260	−8.04266	−8.38092
	A_1	4.04380	4.08689	4.06453	4.39982
	A_2	2.44647	3.32402	2.71992	2.49836
	A_3	−19.95160	−19.94770	−18.16330	−18.41450
	A_4	−4.69736	−7.43701	−7.61441	−8.34188
	A_5	28.52820	29.84090	27.68890	28.32440
	σ	.08	.07	.07	.06
$\Delta\kappa_s/(TPa^{-1})$	A_0	−452.966	−513.048	−544.757	−578.875
	A_1	211.866	225.124	236.304	251.020
	A_2	−75.668	−74.705	−81.628	−84.082
	A_3	−130.578	−109.677	−106.056	−119.775

TABLE 5 (Continued)

A_i	293.15 K	303.15 K	308.15 K	313.15 K
A_4	11.465	−13.902	−15.678	−23.425
A_5	185.052	151.786	151.223	172.576
σ	.80	.58	.58	.54

Note: Standard uncertainties u are $u(T) = .02$ K, $u(p) = .04$ MPa, and the combined expanded uncertainties Uc in mole fraction, density, and speed of sound were $Uc(x) = .0006$, $Uc(\rho) = .0009$ g·cm^{-3}, $Uc(\underline{u}) = 2.63$ m·s^{-1}, respectively (.95 level of confidence).

TABLE 6 Binary parameters and the absolute average deviation for liquid density and speed of sound for all the mixtures considering in the temperature range of 293.15 K to 313.15 K and at .1 MPa.

			%*AADu*	
Mixture	k_{ij}	%*AAD*ρ	**PC-SAFT + SCFT**	**PC-SAFT + NR**
DES (1) + methanol (2)	.3521	.18	.62	1.63
DES (1) + ethanol (2)	.2552	.31	.74	2.01
DES (1) + 1-propanol (2)	.0775	.32	1.99	.32
Overall		.27	1.12	1.32

Note: Standard uncertainties u are $u(T) = .02$ K, $u(p) = .04$ MPa, and the combined expanded uncertainties Uc in mole fraction, density, and speed of sound were $Uc(x) = .0006$, $Uc(\rho) = .0009$ g·cm^{-3}, $Uc(\underline{u}) = 2.63$ m·s^{-1}, respectively (.95 level of confidence).

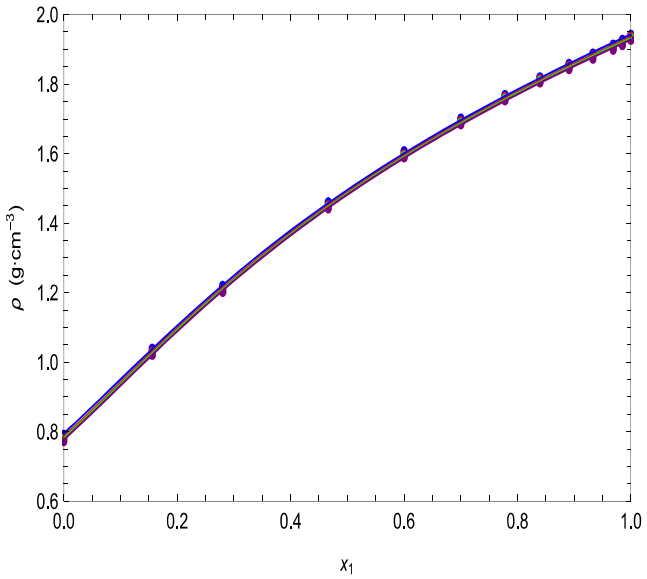

FIGURE 8 Plot of the density for the {[$ZnCl_2$][phosphoric acid] 1:2.5 (x_1) + methanol (x_2)} at different temperatures as a function of the composition expressed in the mole fraction of [$ZnCl_2$][phosphoric acid] 1:2.5 at 293.15 K (blue), 303.15 K (red), 308.15 K (green), and 313.15 K (purple). The lines were generated using perturbed chain statistical associating fluid theory equation of state (PC-SAFT EoS).

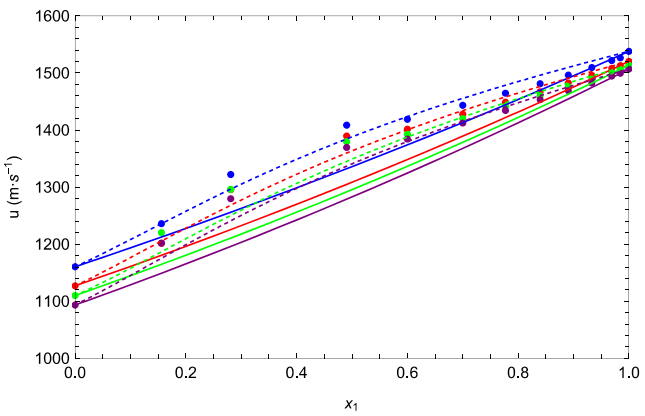

FIGURE 9 Plot of the speed of sound for the {[$ZnCl_2$][phosphoric acid] 1:2.5 (x_1) + ethanol (x_2)} at different temperatures as function of the composition expressed in the mole fraction of [$ZnCl_2$][phosphoric acid at 293.15 K (blue), 303.15 K (red), 308.15 K (green), and 313.15 K (purple). The continuous lines are results obtained with PC-SAFT + NR and the segmented lines are results obtained with PC-SAFT + SCFT.

Figures 4 and 5 with propanol showing the largest deviations. If sigma surface charges shown in Figure 10 The blue color represents the electropositive region hence the H-bond donor part of the molecule whereas the red region denotes the electronegative part or H-bond acceptor of the molecule. Anions have shown favorable interaction with hydrogen bond donor and non-polar groups. Three solutes methanol, ethanol and propanol has shown the same electronegative and electropositive charges as they showed a similar peak in H-bond acceptor and donor regions however due to the difference in the length

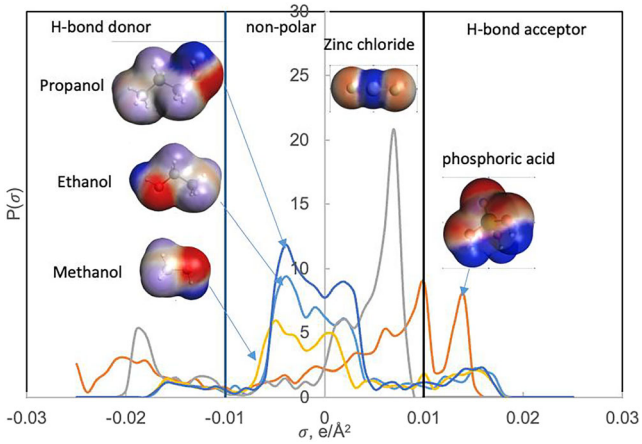

FIGURE 10 Surface charge densities on the COSMO surfaces and sigma profiles generated for [ZnCl2], [H3PO4], methanol, ethanol, and propanol.

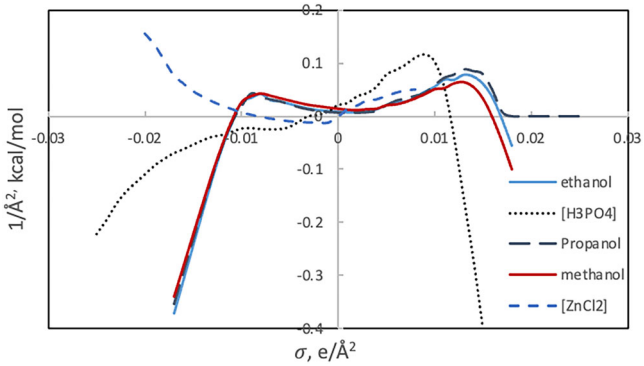

FIGURE 11 Sigma protentials for the chemical spicies used in this study.

of their alkyl chain they have shown different peaks in non-polar region with propanol being the highest and methanol the lowest peaks.

5 | CONCLUSIONS

In this study, the thermophysical properties of the binary mixtures of [$ZnCl_2$][phosphoric acid] 1:2.5 in methanol, ethanol, propanol at T = (293.15, 303.15, 308.15, 313.15) K were measured as a function of temperature and composition. Therefore, thermodynamic relevant parameters such as V_m^E,κ_s, $\Delta\kappa_s$, and L_f have been computed using density and speed of sound to confirm intermolecular interactions which occur in the mixtures. Isentropic compressibility is positive for all systems. This indicates that the mixtures are compressible. A negative excess isentropic compressibility indicates that the mixture is less compressible than ideal behavior would predict. The calculated excess molar volumes for [$ZnCl_2$][phosphoric acid] 1:2.5 in methanol, ethanol, or propanol were negative and positive. The study also clearly shows that the ion-solvent/solute-solvent interaction is dominant over self-interactions such as solvent-solvent/ion-ion/solute-solute. The Redlich-Kister smoothing expression was successfully applied to the correlation of excess molar volumes and excess isentropic compressibility. PC-SAFT EoS modeled DES and alcohol using a 2B scheme. The parameters for the DES as a pseudo-pure fluid were successfully obtained with a deviation of .05% for the density. The overall deviation in density for the mixtures was .27% using PC-SAFT EoS. The smallest overall deviation for the speed of sound was obtained with SCFT (1.12%).

Supporting Information (SI): Supporting Information is available.

Excess molar volumes, V_m^E, and excess isentropic compressibilities $\Delta\kappa_s$, for the binary mixtures {[$ZnCl_2$][phosphoric acid] 1:2.5 (x_1) + methanol, ethanol or propanol (x_2)} at T = (293.15, 303.15, 308.15, and 313.15) K (Table S1); Experimental densities, speed of sound and calculated isentropic compressibilities of the binary mixture of {[$ZnCl_2$][phosphoric acid] 1:2.5 + methanol (a), ethanol (b), and propanol (c)} at T = (293.15, 303.15, 308.15, and 313.15) K (Figures S1–S3).

ACKNOWLEDGEMENTS

The authors wish to acknowledge the North-West University, Materials Science Innovation & Modelling Research Focus Area (MaSIM), National Research Fund (NRF), and Sasol and Chemical Industries Educational and Training Authority (CHIETA). Also, the KSU author acknowledges the funding from Researchers Supporting Project number (RSP2024R355), King Saud University, Riyadh, Saudi Arabia.

ORCID

Indra Bahadur https://orcid.org/0000-0003-2906-473X
Faruq Mohammad https://orcid.org/0000-0002-9318-9986

REFERENCES

1. Zhang Q, Vigier KDO, Royer S, Jérôme F. Deep eutectic solvents: syntheses, properties and applications. *Chem Soc Rev*. 2012;41(21):7108-7146. doi:10.1039/c2cs35178a
2. Hansen BB, Spittle S, Chen B, et al. Deep eutectic solvents: a review of fundamentals and applications. *Chem Rev*. 2020;121(3):1232-1285. doi:10.1021/acs.chemrev.0c00385
3. Zaib Q, Eckelman MJ, Yang Y, Kyung D. Are deep eutectic solvents really green?: a life-cycle perspective. *Green Chem*. 2022;24(20):7924-7930. doi:10.1039/D2GC01752K
4. Omar KA, Sadeghi R. Physicochemical properties of deep eutectic solvents: a review. *J Mol Liq*. 2022;360:119524. doi:10.1016/j.molliq.2022.119524

5. Perna FM, Vitale P, Capriati V. Deep eutectic solvents and their applications as green solvents. *Curr Opin Green Sustain Chem*. 2020;21:27-33. doi:10.1016/j.cogsc.2019.09.004
6. Smith EL, Abbott AP, Ryder KS. Deep eutectic solvents (DESs) and their applications. *Chem Rev*. 2014;114(21):11060-11082. doi:10.1021/cr300162p
7. Hooshmand SE, Afshari R, Ramón DJ, Varma RS. Deep eutectic solvents: cutting-edge applications in cross-coupling reactions. *Green Chem*. 2020;22(12):3668-3692. doi:10.1039/D0GC01494J
8. Shah D, Mjalli FS. Effect of water on the thermo-physical properties of reline: an experimental and molecular simulation based approach. *PCCP*. 2014;16(43):23900-23907. doi:10.1039/C4CP02600D
9. Lapeña D, Bergua F, Lomba L, Giner B, Lafuente C. A comprehensive study of the thermophysical properties of reline and hydrated reline. *J Mol Liq*. 2020;303:112679. doi:10.1016/j.molliq.2020.112679
10. Paredes X, Queirós C, Santos F, et al. Thermophysical properties of 1-hexyl-3-methylimidazolium bis (trifluoromethylsulfonyl) imide,[C6mim][(CF3SO2) 2N]—new data, reference data, and reference correlations. *J Phys Chem Ref Data Monogr*. 2020;49(4):043101. doi:10.1063/5.0023160
11. Poling BE, Prausnitz JM, O'connell JP. *Properties of gases and liquids*. McGraw-Hill Education; 2001.
12. Yang W, Du X, Zhao J, et al. Hydrated eutectic electrolytes with ligand-oriented solvation shells for long-cycling zinc-organic batteries. *Joule*. 2020;4(7):1557-1574. doi:10.1016/j.joule.2020.05.018
13. Ni Q, Kim B, Wu C, Kang K. Non-electrode components for rechargeable aqueous zinc batteries: electrolytes, solid-electrolyte-interphase, current collectors, binders, and separators. *Adv Mater*. 2022;34(20):2108206. doi:10.1002/adma.202108206
14. Walvekar R, Saputra R, Khalid M, Vaka M, Mubarak NM, Dharaskar S. Thermophysical properties of novel ammonium-based eutectic solvents with ethane-1, 2-diol and ZnCl2. *J Chem Technol Biotechnol*. 2022;97(10):2728-2738. doi:10.1002/jctb.7138
15. Bernasconi R, Panzeri G, Accogli A, Liberale F, Nobili L, Magagnin L. Electrodeposition from deep eutectic solvents, Intech. *Prog Dev Lon Liq*. 2017;235-261. doi:10.5772/64935
16. Xiong J, Yu S, Zhu H, Wang S, Chen Y, Liu S. Dissolution and structure change of bagasse cellulose in zinc chloride solution. *BioResources*. 2016;11(2):3813-3824. doi:10.15376/biores.11.2.3813-3824
17. Wang Y, Niu Z, Zheng Q, et al. Zn-based eutectic mixture as anolyte for hybrid redox flow batteries. *Sci Rep*. 2018;8(1):5740. doi:10.1038/s41598-018-24059-x
18. Marset X, Guillena G. Deep eutectic solvents as à-la-carte medium for transition-metal-catalyzed organic processes. *Molecules*. 2022;27(23):8445. doi:10.3390/molecules27238445
19. Mgxadeni N, Mmelesi O, Kabane B, Bahadur I. Influence of hydrogen bond donor on zinc chloride in separation of binary mixtures: activity coefficients at infinite dilution. *J Mol Liq*. 2022;351:118596. doi:10.1016/j.molliq.2022.118596
20. Munjal S, Singh A. *The Arrhenius acid and base theory, corrosion*. IntechOpen; 2020.
21. Lower SK. *Introduction to acid-base chemistry, a Chem1 reference text*. Simon Fraser University; 1999.
22. Ebbing D, Gammon SD. *General chemistry*. Cengage Learning; 2016.
23. Gilli P, Pretto L, Bertolasi V, Gilli G. Predicting hydrogen-bond strengths from acid− base molecular properties. The p K a slide rule: toward the solution of a long-lasting problem. *Acc Chem Res*. 2009;42(1):33-44. doi:10.1021/ar800001k
24. Koolman J, Röhm K-H, Wirth J, Robertson M. *Color atlas of biochemistry*; 2005. doi:10.1055/b-005-148878
25. Zhao N, Liu K, He C, et al. H3PO4 activation mediated the iron phase transformation and enhanced the removal of bisphenol a on iron carbide-loaded activated biochar. *Environ Pollut*. 2022;300:118965. doi:10.1016/j.envpol.2022.118965
26. Redlich O, Kister A. Algebraic representation of thermodynamic properties and the classification of solutions. *Ind Eng Chem*. 1948;40(2):345-348. doi:10.1021/ie50458a036
27. Jindal A, Vasudevan S. Hydrogen bonding in the liquid state of linear alcohols: molecular dynamics and thermodynamics. *J Phys Chem B*. 2020;124(17):3548-3555. doi:10.1021/acs.jpcb.0c01199
28. Venkatesu P. Thermophysical contribution of N, N-dimethylformamide in the molecular interactions with other solvents. *Fluid Phase Equilib*. 2010;298(2):173-191. doi:10.1016/j.fluid.2010.07.010
29. Ramkumar V, Gardas RL. Exploring the solvation behavior of guanidinium based carboxylate ionic liquids in DMSO and DMF through apparent molar properties. *J Mol Liq*. 2021;343:117664. doi:10.1016/j.molliq.2021.117664
30. Gonzalez-Miquel M, Massel M, DeSilva A, Palomar J, Rodriguez F, Brennecke JF. Excess enthalpy of monoethanolamine + ionic liquid mixtures: how good are COSMO-RS predictions? *J Phys Chem B*. 2014;118(39):11512-11522. doi:10.1021/jp507547q
31. Kumar N, Naik PK, Banerjee T. Molecular dynamic insights into the distinct solvation structures of aromatic and aliphatic compounds in Monoethanolamine-based deep eutectic solvents. *J Phys Chem B*. 2022;126(2022):4925-4938. doi:10.1021/acs.jpcb.2c01735
32. Xu H, Kong Y, Peng J, Wang W, Li B. Mechanism of deep eutectic solvent delignification: insights from molecular dynamics simulations. *ACS Sus Chem Eng*. 2021;9(20):7101-7111. doi:10.1021/acssuschemeng.1c01260
33. Hoga HE, Olivieri GV, Torres RB. Experimental measurements of volumetric and acoustic properties of binary mixtures of 1-Butyl-3-methylimidazolium hexafluorophosphate with molecular solvents. *J Chem Eng Data*. 2020;65(7):3406-3419. doi:10.1021/acs.jced.9b01032
34. Bittencourt SS, Hoga HE, Torres RB, d'Angelo JVH. Thermodynamic and spectroscopic properties of binary mixtures of n-butylammonium butanoate ionic liquid with alcohols at T= (293.15–313.15) K. *J Chem Thermodyn*. 2017;105:238-252. doi:10.1016/j.jct.2016.09.007
35. Negadi L, Feddal-Benabed B, Bahadur I, et al. Effect of temperature on density, sound velocity, and their derived properties for the binary systems glycerol with water or alcohols. *J Chem Thermodyn*. 2017;109:124-136. doi:10.1016/j.jct.2017.01.011
36. Naseem B, Iftikhar M. Investigation on molecular interactions of antibiotics in alcohols using volumetric and acoustic studies at different temperatures. *J Chem Thermodyn*. 2017;104:239-251. doi:10.1016/j.jct.2016.09.037

37. Chen J, Chen L, Xu Y. Properties of pure 1, 1, 3, 3-tetramethylguanidine imidazole ionic liquid and its binary mixtures with alcohols at T=(293.15 to 313.15) K. *J Chem Thermodyn*. 2015;88:110-120. doi:10.1016/j.jct.2015.04.027
38. Naseem B. Effect of alkyl chain length of 1-alkanols on solution behavior of bactericidal antibiotic in terms of thermo-acoustic parameters. *J Mol Liq*. 2020;307:112991. doi:10.1016/j.molliq.2020.112991
39. Valtz A, Teodorescu M, Wichterle I, Richon D. Liquid densities and excess molar volumes for water + diethylene glycolamine, and water, methanol, ethanol, 1-propanol + triethylene glycol binary systems at atmospheric pressure and temperatures in the range of 283.15–363.15 K. *Fluid Phase Equilib*. 2004;215(2):129-142. doi:10.1016/S0378-3812(03)00364-9
40. Xu Y, Chen B, Qian W, Li H. Properties of pure n-butylammonium nitrate ionic liquid and its binary mixtures of with alcohols at T=(293.15 to 313.15) K. *J Chem Thermodyn*. 2013;58:449-459. doi:10.1016/j.jct.2012.10.008
41. Benkelfat-Seladji NL, Ouaar F, Hernández A, et al. Density, speed of sound, refractive index of binary mixtures containing 2-ethoxyethanol and some alcohols: measurement and correlation. *J Chem Thermodyn*. 2022;170:106762. doi:10.1016/j.jct.2022.106762
42. Kumar PK, Kabanda MM, Bahadur I, Venkatesu P, Ebenso EE. Influence of temperature and concentration on the molecular interactions of pyrrolidinium-based ionic liquid with water and alcohols: an experimental and DFT studies. *J Mol Liq*. 2022;360:119554. doi:10.1016/j.molliq.2022.119554
43. Nduli M, Deenadayalu N. Thermophysical properties of binary mixtures of (methanol or 1-ethyl-3-methylimidazolium acetate + furfural or furfuryl alcohol) at various temperatures. *J Mol Liq*. 2017;241:407-421. doi:10.1016/j.molliq.2017.06.029
44. Singh S, Aznar M, Deenadayalu N. Densities, speeds of sound, and refractive indices for binary mixtures of 1-butyl-3-methylimidazolium methyl sulphate ionic liquid with alcohols at T=(298.15, 303.15, 308.15, and 313.15) K. *J Chem Thermodyn*. 2013;57:238-247. doi:10.1016/j.jct.2012.08.030
45. Bahadur I, Deenadayalu N, Ramjugernath D. Effects of temperature and concentration on interactions in methanol+ ethyl acetate and ethanol+ methyl acetate or ethyl acetate systems: insights from apparent molar volume and apparent molar isentropic compressibility study. *Thermochim Acta*. 2014;577:87-94. doi:10.1016/j.tca.2013.12.016
46. Li Z, Zhao D, Zhuang Y, Yang F, Liu X, Chen Y. Volumetric properties of monoethanolamine and alcohol binary mixtures at different temperatures and 0.1 MPa. *J Chem Thermodyn*. 2019;133:37-45. doi:10.1016/j.jct.2019.01.025
47. García-Abuín A, Gomez-Diaz D, La Rubia M, Navaza J. Density, speed of sound, viscosity, refractive index, and excess volume of N-methyl-2-pyrrolidone + ethanol (or water or ethanolamine) from T=(293.15 to 323.15) K. *J Chem Eng Data*. 2011;56(3):646-651. doi:10.1021/je100967k
48. Zhu C, Han S, Liu J, Ma Y. Densities and viscosities of Diaminotoluene with water, ethanol, Propan-1-ol, and Butan-1-ol from (293.15 to 333.15) K. *J Chem Eng Data*. 2014;59(3):880-889. doi:10.1021/je400968v
49. Bahadur I, Deenadayalu N. Apparent molar volume and apparent molar isentropic compressibility for the binary systems {methyltrioctylammoniumbis (trifluoromethylsulfonyl) imide+ ethyl acetate or ethanol} at different temperatures under atmospheric pressure. *Thermochim Acta*. 2013;566:77-83. doi:10.1016/j.tca.2013.05.015
50. Li D, Guo M, Wu Q, Li M, Ruan N, Gao L. Investigations on the Thermophysical properties of the binary mixtures of ethyl laurate with four n-alkanols. *J Solution Chem*. 2020;49(9-10):1237-1249. doi:10.1007/s10953-020-01024-9
51. Bahadur I, Kgomotso M, Ebenso EE, Redhi G. Influence of temperature on molecular interactions of imidazolium-based ionic liquids with acetophenone: thermodynamic properties and quantum chemical studies. *RSC Adv*. 2016;6(106):104708-104723. doi:10.1039/C6RA15476J
52. Masilo K, Bahadur I. Intermolecular interactions between 1-Ethyl-3-methylimidazolium-based ionic liquids with carboxylic acid at different temperatures via thermodynamic and spectroscopic studies. *J Chem Eng Data*. 2021;66(3):1211-1230. doi:10.1021/acs.jced.0c00728
53. Kabane B, Chokkareddy R, Redhi GG. Molecular interaction studies of binary systems comprising [C2mim][BF4] with ethyl acetoacetate or benzaldehyde. *Heliyon*. 2019;5(5):e01548. doi:10.1016/j.heliyon.2019.e01548
54. Fortin TJ, Laesecke A, Freund M, Outcalt S. Advanced calibration, adjustment, and operation of a density and sound speed analyzer. *J Chem Thermodyn*. 2013;57:276-285. doi:10.1016/j.jct.2012.09.009
55. Gross J, Sadowski G. Perturbed-chain SAFT: an equation of state based on a perturbation theory for chain molecules. *Ind Eng Chem Res*. 2001;40(4):1244-1260. doi:10.1021/ie0003887
56. Gross J, Sadowski G. Application of the perturbed-chain SAFT equation of state to associating systems. *Ind Eng Chem Res*. 2002;41(22):5510-5515. doi:10.1021/ie010954d
57. Schaaffs W. The problem of a theoretical calculation of the velocity of sound for binary liquid mixtures. *Acta Acust United Acust*. 1975;33:272-276.
58. Nomoto O. Empirical formula for sound velocity in liquid mixtures. *J Physical Soc Japan*. 1958;13(12):1528-1532. doi:10.1143/JPSJ.13.1528
59. Squire TH, Marschall J. Material property requirements for analysis and design of UHTC components in hypersonic applications. *J Eur Ceram Soc*. 2010;30(11):2239-2251. doi:10.1016/j.jeurceramsoc.2010.01.026
60. Chiappe C, Pieraccini D. Ionic liquids: solvent properties and organic reactivity. *J Phys Org Chem*. 2005;18(4):275-297. doi:10.1002/poc.863
61. Silva LP, Martins MA, Conceição JOH, Pinho SP, Coutinho JA. Eutectic mixtures based on polyalcohols as sustainable solvents: screening and characterization, ACS sustain. *Chem Eng*. 2020;8(40):15317-15326. doi:10.1021/acssuschemeng.0c05518
62. Fatima U, Dhakal P, Shah JK. Comparative study of influence of ethanol and 2, 2, 2-trifluoroethanol on thermophysical properties of 1-ethyl-3-methylimidazolium dicyanamide in binary mixtures: experimental and MD simulations. *J Chem Eng Data*. 2020;66(1):101-115. doi:10.1021/acs.jced.0c00447
63. Bhattarai A, Chatterjee SK, Niraula TP. Effects of concentration, temperature and solvent composition on density and apparent molar volume of the binary mixtures of cationic-anionic surfactants in methanol–water mixed solvent media. *SpringerPlus*. 2013;2(1):280. doi:10.1186/2193-1801-2-280

64. Linder CJ. University physics students' conceptualizations of factors affecting the speed of sound propagation. *Int J Sci Educ*. 1993;15(6):655-662. doi:10.1080/0950069930150603
65. Dzida M, Zorebski E, Zorębski M, et al. Speed of sound and ultrasound absorption in ionic liquids. *Chem Rev*. 2017;117(5):3883-3929. doi:10.1021/acs.chemrev.5b00733
66. Brocos P, Piñeiro Á, Bravo R, Amigo A. Refractive indices, molar volumes and molar refractions of binary liquid mixtures: concepts and correlations. *PCCP*. 2003;5(3):550-557. doi:10.1039/b208765k
67. Letcher TM, Redhi GG. Phase equilibria for liquid mixtures of (butanenitrile + a carboxylic acid + water) at 298.15 K. *Fluid Phase Equilib*. 2002;193(1-2):123-133. doi:10.1016/S0378-3812(01)00640-9
68. Leron RB, Soriano AN, Li M-H. Densities and refractive indices of the deep eutectic solvents (choline chloride + ethylene glycol or glycerol) and their aqueous mixtures at the temperature ranging from 298.15 to 333.15 K. *J Taiwan Inst Chem Eng*. 2012;43(4):551-557. doi:10.1016/j.jtice.2012.01.007
69. Masilo K, Bahadur I. Investigation on the molecular interaction of binary mixtures of acetophenone with carboxylic acids at various temperature: thermodynamic and spectroscopic aspects. *J Chem Thermodyn*. 2022;166:106667. doi:10.1016/j.jct.2021.106667
70. Bhanuprakash P, Gardas RL, Prathibha R, Sivakumar K, Jyothi N. Insights into non-ideal behaviour of benzyl alcohol with (C2-C4) carboxylic acids through volumetric, ultrasonic and ATR-FTIR spectroscopic studies. *Phys Chem Liq*. 2021;59(4):632-654. doi:10.1080/00319104.2020.1808654
71. Bhanuprakash P, Prathibha R, Gardas RL, Sivakumar K, Jyothi N. Effect of temperature, nature of anion and alkyl chain length on the volumetric and acoustic properties of ionic liquid [C4C1im][MeSO4] with alkyl nitriles. *J Mol Liq*. 2020;302:112507. doi:10.1016/j.molliq.2020.112507
72. Zhao L, Zhang J. Intermolecular interaction of diamine-diol binary system: a mini-review. *Adv Colloid Interface Sci*. 2022;102662:102662. doi:10.1016/j.cis.2022.102662
73. Piehl J, Samimi-Abianeh O. Measuring the adiabatic ignition delay of n-pentane mixture using rapid compression machine. *J Therm Sci*. 2020;1-9(2):552-560. doi:10.1007/s11630-020-1346-7
74. Zafarani-Moattar MT, Shekaari H. Apparent molar volume and isentropic compressibility of ionic liquid 1-butyl-3-methylimidazolium bromide in water, methanol, and ethanol at T = (298.15 to 318.15) K. *J Chem Thermodyn*. 2005;37(10):1029-1035. doi:10.1016/j.jct.2005.01.009
75. Gowrisankar M, Venkateswarlu P, Sivakumar K, Sivarambabu S. Ultrasonic studies on molecular interactions in binary mixtures of N-methyl aniline with methyl isobutylketone + 3-pentanone, and + cycloalkanones at 303.15 K. *J Solution Chem*. 2013;42(5):916-935. doi:10.1007/s10953-013-0003-0
76. Astbury G, Hawksworth SJ. Spontaneous ignition of hydrogen leaks: a review of postulated mechanisms. *Int J Hydrogen Energy*. 2007;32(13):2178-2185. doi:10.1016/j.ijhydene.2007.04.005
77. Knoerzer K, Buckow R, Sanguansri P, Versteeg C. Adiabatic compression heating coefficients for high-pressure processing of water, propylene-glycol and mixtures–a combined experimental and numerical approach. *J Food Eng*. 2010;96(2):229-238. doi:10.1016/j.jfoodeng.2009.07.017
78. Venkatramana L, Sreenivasulu K, Sivakumar K, Dayananda Reddy K. Thermodynamic properties of binary mixtures containing 1-alkanols. *J Therm Anal Calorim*. 2014;115(2):1829-1834. doi:10.1007/s10973-013-3473-9
79. Bahadur I, Deenadayalu N, Naidoo P, Ramjugernath D. Density, speed of sound, and refractive index measurements for the binary systems (butanoic acid + propanoic acid, or 2-methylpropanoic acid) at T = (293.15 to 313.15) K. *J Chem Thermodyn*. 2013;57:203-211. doi:10.1016/j.jct.2012.07.019

SUPPORTING INFORMATION

Additional supporting information can be found online in the Supporting Information section at the end of this article.

How to cite this article: Mgxadeni N, Kabane B, Hernández A, et al. Application of PC-SAFT EoS and SCFT for the modeling of thermophysical properties comprising deep eutectic solvent and alcohols. *Asia-Pac J Chem Eng*. 2024;19(3):e3031. doi:10.1002/apj.3031